Received July 14, 2019, accepted August 16, 2019, date of publication August 21, 2019, date of current version September 6, 2019.

Digital Object Identifier 10.1109/ACCESS.2019.2936656

Application of Different Optimization Algorithms for Optimal Sizing of PV/Wind/Diesel/Battery Storage Stand-Alone Hybrid Microgrid

AHMED A. ZAKI DIAB[1,2], HAMDY M. SULTAN[2], IHAB S. MOHAMED[3], KUZNETSOV OLEG N.[4], AND TON DUC DO[5], (Member, IEEE)

[1]Department of Electrical and Electronic Engineering, Kyushu University, Fukuoka 819-0395, Japan
[2]Electrical Engineering Department, Faculty of Engineering, Minia University, Minia 61111, Egypt
[3]INRIA Sophia Antipolis - Méditerranée, University Côte d'Azur, 06100 Nice, France
[4]Electrical Power Systems Department, Moscow Power Engineering Institute (MPEI), 111250 Moscow, Russia
[5]Department of Robotics and Mechatronics, School Engineering and Digital Sciences (SEDS), Nazarbayev University, Nur-Sultan Z05H0P9, Kazakhstan

Corresponding authors: Ahmed A. Zaki Diab (a.diab@mu.edu.eg) and Ton Duc Do (doduc.ton@nu.edu.kz)

This work was supported by Nazarbayev University through the NU-ORAU Program, under Grant 06/06.17.24.

ABSTRACT In this paper, a simulation model describing the operation of a PV/wind/diesel hybrid microgrid system with battery bank storage has been proposed. Optimal sizing of the proposed system has been presented to minimize the cost of energy (COE) supplied by the system while increasing the reliability and efficiency of the system presented by the loss of power supply probability (LPSP). Novel optimization algorithms of Whale Optimization Algorithm (WOA), Water Cycle Algorithm (WCA), Moth-Flame Optimizer (MFO), and Hybrid particle swarm-gravitational search algorithm (PSOGSA) have been applied for designing the optimized microgrid. Moreover, a comprehensive comparison has been accomplished between the proposed optimization techniques. The optimal sizing of the system components has been carried out using real-time meteorological data of Abu-Monqar village located in the Western Desert of Egypt for the first time for developing this promising remote area. Statistical study for determining the capability of the optimization algorithm in finding the optimal solution has been presented. Simulation results confirmed the promising performance of the hybrid WOA over the other algorithms.

INDEX TERMS Isolated microgrids, cost of energy (COE), loss of power supply probability (LPSP), optimization.

ACRONYMS AND ABBREVIATIONS

COE	Cost of Energy
WOA	Whale Optimization Algorithm
WCA	Water Cycle Algorithm
MFO	Moth-Flame Optimizer
PSOGSA	Hybrid particle Swarm-Gravitational Search Algorithm
LPSP	Loss of Power Supply Probability
RES	Renewable Energy Systems
GA	Genetic Algorithm
PSO	Particle Swarm Optimization
SA	Simulated Annealing Optimization
RSM	Response Surface Methodology
MOPSO	Multi-Objective Particle Swarm Optimization
SOO	Single Objective Optimization
ELF	Equivalent Loss Factor
PS	Pattern Search Optimizer
SMCS	sequential Monte Carlo Simulation
MOSaDE	Multi-Objective Self-Adaptive Differential Evolution
HOMER	Hybrid Optimization of Multiple Energy Resources
NASA	National Aeronautics and Space Administrative
n_{PV} *and* n_{WT}	Number PV Modules and Wind Turbines, respectively
P_{PV_rated}	Rated Power of the PV Module

The associate editor coordinating the review of this manuscript and approving it for publication was Nishad Mendis.

η_{PV}, η_{WT}, *and* η_{wire}	The efficiency of the PV Module, Wind Turbine, and Wires, respectively
$G(t)$ *and* G_{nom}	Solar Radiation Intensity at time t and under Standard Conditions, respectively
β_T	Temperature Coefficient of the PV Module
T_c (t) *and* T_{nom}	Cell Temperature at time t and under Standard Conditions, respectively
u_1 *and* u_2	Wind Speed at the Reference Point h_1 and Turbine Hub with Height h_2, respectively
P_{WT} *and* P_{R_WT}	The Actual Power Generated from a Wind Turbine and its Rated Power, respectively
$u(t)$, u_{cut-in}, u_{rated}, u_{cut_off}	Wind Speed at time t, Cut-in Wind Speed, Wind Speed at Rated Power, and Cut-off Wind Speed, respectively
DOD	Depth of Discharge
SOC	State of Charge of the Battery Storage System
Σ	Self-discharge Rate
E_{CH} (t) *and* $E_{DIS}(t)$	Charging and Discharging Energy at time t
$P_{load}(t)$	Load Power at time t
η_{conv}, η_{CH}, η_{DIS}	The efficiency of the converter, battery charging, and discharging, respectively
Δt	Time interval = 1hour
DG	Diesel Generator
$D_f(t)$	Fuel consumption of the diesel generator at time t
P_{DG} (t) *and* P_{DG_R}	The power generated from DG at time t and its rated capacity, respectively
α_{DG} & β_{DG}	coefficients of the fuel consumption curve of the DG
$P_{dummy}(t)$	Power consumed in the dummy load at time t
NPC	Net present cost
C_{ann_tot}	The annual cost of investment
C_{ann_cap}, C_{ann_rep}, C_{ann_oper}, *and* C_{ann_maint}	Annual capital, replacements, operating, and maintenance cost for the components, respectively.
CRF	Capital recovery factor
r	Rate of interest
n	A lifetime of the whole project
C_{cap_PV}, C_{cap_WT}, C_{cap_batt}, C_{cap_DG}, *and* C_{cap_conv}	The initial capital cost of installation of the PV system, wind system, battery bank, and the diesel generator, and converter, respectively
$C_{ann\_cap\_PV}$, $C_{ann\_cap\_WT}$, $C_{ann\_cap\_batt}$, $C_{ann\_cap\_DG}$, *and* $C_{ann\_cap\_conv}$	Annual interest of capital cost of the PV system, wind system, battery bank, and the diesel generator, and converter, respectively
M_{PV}, M_{WT}, M_{batt}, M_{DG}, *and* M_{conv}	A lifetime of PV modules, wind turbines, battery banks, diesel generator, and converter, respectively.
$C_{oper\&main\_PV}$, $C_{oper\&main\_wind}$, $C_{oper\&main\_batt}$, $C_{oper\&main\_conv}$, *and* $C_{oper\&main\_DG}$	Operating and maintenance cost of PV, wind turbine, battery banks, converter, and diesel generator per unit time, respectively.
t_{PV}, t_{WT}, t_{batt}, t_{conv}, *and* t_{DG}	The operating time of PV, wind turbine, battery banks, converter, and diesel generator, respectively.
K_{C_rep}	The capacity of the units used in the system
C_u	The cost of the replaced units
n_{rep}	Number of replacements over the project lifetime n
$\vec{X}^*$ *and* $\vec{X}$	Vectors describing the best position and the current position of whales, respectively
$\vec{r}_1$ *and* $\vec{r}_2$	Random vectors between [0, 1]
b	Constant number for determining the shape the spiral
l	A random number between $[-1, 1]$
A *and* C	coefficient vectors
$\vec{X}^i_{stream}(t)$, $\vec{X}^i_{river}(t)$, *and* $\vec{X}^i_{sea}(t)$	The current positions of the streams, rivers, and sea, respectively
$\vec{X}^i_{stream}(t+1)$ *and* $\vec{X}^i_{river}(t+1)$	The new positions of the streams and rivers, respectively
rand	arbitrarily number distributed uniformly between [0, 1]
P_{best} *and* g_{best}	The personal best and the global best positions, respectively

$v_i\,(n)$ *and* $v_i\,(n+1)$	speed of "ith" particle in the iteration n and n+1, respectively
w	inertia weight
$x_i\,(n)$ *and* $x_i\,(n+1)$	represents the present position of the "ith" particle in the iterations n and n+1, respectively
x_i, M_{ii}, M_{ai}, *and* M_{ip}.	The position, mass of inertia, active gravitational mass, and the passive gravitational mass of the object, respectively
G_O *and* $G(t)$	The initial value of gravitational constant and gravitational constant at a specified time "t", respectively
$R_{ij}(t)$	Euclidian spacing between the two candidates i and j
$F_i^d(t)$	The total force influencing on the agent i
$ac_i^d(t)$	Acceleration of candidate agent i
M *and* F	Matrix introduces the set of generated moths and Flames, respectively
OM *and* OF	Matrix for storing the fitness values of the moths and flames, respectively
$S(M_i, F_j)$	The spiral function of the i-th moth for the j-th flame
D_i	The distance of the i-th moth for the j-th flame

I. INTRODUCTION

A. MOTIVATION AND INCITEMENT

Despite the significant increases in the development of global renewable energy technology, electricity shortages remain a serious problem in rural areas and islands with large sources of renewable energy. Meanwhile, in the last years, enhanced power electronics have been used to support renewable energy sources (RES) to frugally supply electric energy for comprehensive range applications. The high specific cost of the generated units from RES, when compared with that from the traditional power plants, and the availability of renewable energy sources, are the two main challenges for the implementation of RES in large scale, as introduced in [1]. Moreover, due to the intermittent nature of almost renewable sources, the feasibility of high RES sharing can be increased, considering energy mix from different types of renewable resources side by side with the application of energy storage system. The previously mentioned challenges lead the decision-makers to think about the combination of conventional energy sources with RES as a hybrid microgrid system in order to increase the share of RES in the energy mix [2]. Microgrid power systems, including photovoltaic and wind energy, hybrid with diesel generators are investigated, to be a promising energy source and feasible from the economic point of view. Isolated communities, with respect to the supply of electricity, are often located in islands, rural and some urban areas in developing countries. The demand for electricity in these areas is usually provided by diesel generators, leading to considerable uncertainty because of the cost of fuel and the high pollution of the surrounding environment [3]. Therefore, hybrid microgrids can be particularly suitable solution for isolated communities, however, this area still needs to further research, feasibility studies and technological developments.

The total installed capacity of power plants connected into the utility grid in Egypt reached 38.857 GW by the end of 2016 [4]. Abu Monqar is one of the most promising investment areas in the New Valley, Western Desert. The demand for electricity in this area is covered by a diesel generating station including three diesel generator units with capacities ranging from 400 to 660 kW. The average load demand for the isolated village and its surrounding villages is about 265kW [5]. Taking into account the plan of the national energy sector regarding the utilization of renewable resources, which planned to be increased to 20% up to 2027 [6]. Wind turbines and PV are the top two most promising energy resources used in Egypt. Therefore, a certain number of feasibility studies and researches have been presented related to the assessment of the energy potentials and the optimal allocation of these sources in many locations over the territory of the country [6]–[8].

B. LITERATURE REVIEW

Many advanced optimization techniques for the optimal design of hybrid RES has been presented in many research studies in the literature. In [9], [10], the optimal sizing of a PV/wind/diesel hybrid system was presented using Strength Pareto evolutionary algorithm by formulating two objective functions, minimization of system cost and greenhouse gases emissions. In [11]–[13], Genetic algorithm (GA) was used for optimal sizing and configuration of a hybrid PV/wind power system with battery storage under different objective functions; the reliability of the system under weather conditions variations, minimizing the annual cost of the system and to minimize the loss of power supply probability (LPSP). Particle Swarm Optimization (PSO) has been used in many research studies for optimal sizing of hybrid renewable energy systems [14]–[16].

A PV/wind/diesel/battery banks hybrid system was presented in [14]. The uncertainty in the generation of PV and wind energy are considered in [15]. In [16], PSO was used to find the global optimum solution while considering the uncertainty in wind generation within a certain reliability index in PV/wind microgrid system with fuel cells, electrolyzer, hydrogen tank, and battery system. Simulated Annealing (SA) optimization strategy was used for optimal sizing of hybrid PV/wind energy conversion system, while the objective function was to minimize the total energy cost of the hybrid system [17]. The response surface methodology (RSM) was used for optimizing the size of an autonomous PV/wind system with energy storage in some studies [18]. The results obtained from RSM optimization were confirmed using autonomy analysis and loss of load probability, then the

results of this work were used in [17] to be compared with the results obtained from simulated annealing optimization. In [19], mathematical models of hybrid wind and PV systems were developed and multi-objective optimization using PSO and GA were performed.

In [20], Particle swarm optimization has been used for optimal sizing and operation of a PV/wind/battery storage hybrid energy system for minimizing the energy cost over the whole lifetime of the project. The optimization results are compared with GA, where PSO technique proved its superiority in solving the optimization problem in terms of the convergence, speed, and accuracy. In [21], [22], Multi-Objective Particle Swarm Optimization (MOPSO) has been used for the optimal configuration of a hybrid PV/wind microgrid with hydrogen storage for minimizing the cost of energy generated from such a system, taking into account the reliabilities of the system components and outage probabilities of the subsystems. The optimization results have been compared with that of Single Objective Optimization method and Equivalent Loss Factor (ELF) is chosen as the reliability constraint in the optimization problem. In [23], Pattern Search (PS) optimizer and sequential M99onte Carlo Simulation (SMCS) are combined to obtain the minimum total cost of the system and satisfy the reliability requirements from the consumer side.

A comparison with a hybrid GA-SMCS was also performed, from which the PS-SMCS gave a better performance. In [24], cuckoo search optimization algorithm has been used for optimal sizing of an isolated PV/wind/diesel/ battery energy system, while the proposed technique provided high accuracy compared to GA and PSO. Multi-Objective Self-Adaptive Differential Evolution (MOSaDE) algorithm has been used for optimal sizing and operation of a hybrid PV/wind/diesel microgrid system with battery storage for the city of Yanbu, Saudi Arabia, whereas, the multi-objective optimization approach is used to reduce the computational time [25]. The optimal sizing and placement of a grid-connected PV-wind-battery storage microgrid using Artificial Bee Colony optimization technique are presented in [26], while the IEEE 30-bus system was used for the application of the optimal operation. In [27], [28], the Hybrid Optimization of Multiple Energy Resources (HOMER) software has been used for optimum sizing of hybrid wind/PV/diesel system in Malaysia in which the weather conditions, maximum availability and minimum cost were considered.

C. CONTRIBUTION AND PAPER ORGANIZATION

Proceeding from the necessity to diversify electricity generation by giving priority to optimizing the use of renewable energy, this paper investigates on the economical design of a grid-independent hybrid PV/wind power system with battery storage and diesel generator. In this way, Whale Optimization Algorithm (WOA), Water Cycle Algorithm (WCA), Moth-Flame Optimizer (MFO), and Hybrid particle swarm-gravitational search algorithm (PSOGSA) have been exploited for minimizing the cost of energy (COE) generated from this system over its 25 years' lifetime, and subjected to reliability constraints in the form of loss of power supply probability. Concerning the data of solar radiation and wind speed acquired from Abu-Monqar village in Western Desert of Egypt, they are available, based on; (i) the data obtained from National Aeronautics and Space Administrative (NASA), and (ii) the long-term average of meteorological parameters of 20 years of observation. The system cost includes the annual interest of capital investment cost, operation and maintenance, and replacement cost.

The main contributions of the work described in this paper can be summarized as follows:

1. To the best of the authors' knowledge, the proposed optimization algorithms, which are WOA, WCA, MFO, and PSOGSA, have not been reported in the literature for tackling the problem of designing the RES microgrids. Consequently, a comprehensive comparison between these algorithms has been introduced in conjunction with a clear discussion and analysis.
2. Moreover, the objective function proposed in this paper, for determining the best optimal size of the components of the RES microgrid, is novel and different from the conventional objective functions, leading to notable improvements in the system's performance, as illustrated in Section V.
3. Broadly speaking, to the best of the authors' knowledge, this is the first attempt to apply the proposed optimization techniques, to optimize the system components, for solving a real problem of power shortage in Abu-Monqar village located in Western Sahara in Egypt, based on a real-time meteorological data of the site for developing this promising remote area.

The paper is organized as follow: Section II briefly describes the subsystems of the hybrid system. The corresponding models for the subsystems are presented in section III. The energy management strategy is demonstrated in Section IV. Optimization problem statement and the proposed optimization techniques are discussed in Sections V and VI, respectively. A case study is formulated in section VII. Simulation results and discussions are summarized in Section VIII. Statistical analysis is performed in section IX. Finally, Section X is devoted to the conclusion.

II. STAND-ALONE HYBRID MICROGRID ENERGY SYSTEM

Hybrid microgrid power system is the optimum solution for solving the problem of electrification in islands and remote areas where the extension of the transmission networks not economical or a waste of time. Hybrid systems use a combination of several renewable sources of energy such as photovoltaic and wind energy with the battery storage system and diesel generators. Wind turbines and PV modules, when hybridized, supply electric power with higher reliability than that obtained from any one of them individually. Moreover, hybrid systems also allow the installation of smaller and less costly units than that would be used if the system is completely depending on one kind of renewable energy. In this work, the proposed hybrid microgrid system

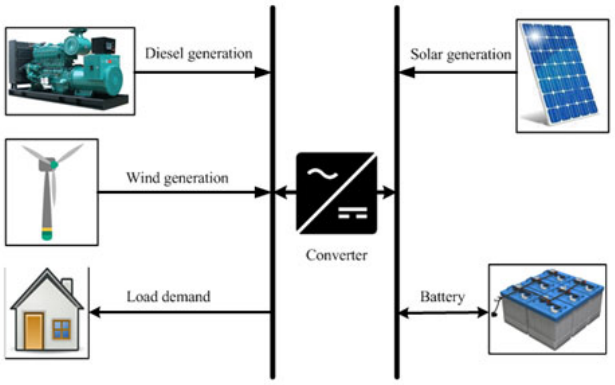

FIGURE 1. Schematic configuration of the proposed hybrid microgrid system.

under study includes five main components; wind turbine, PV modules, diesel generator, inverter, and battery storage. A PV/wind/diesel hybrid system can be a cost-effective solution for solving the problem of electricity in Abu-Monqar. The schematic configuration of the proposed Hybrid microgrid system is shown in Fig. 1. In fact, a PV/Wind/diesel hybrid system can be a cost-effective solution for solving the problem of electricity in Abu-Monqar village.

III. MODELLING OF THE HYBRID MICROGRID WITH PV/WIND/DIESEL/BATTERY GENERATING SYSTEM

A. MODELLING OF THE SOLAR PV SYSTEM

The energy obtained from a PV module in terms of the solar radiation and the ambient temperature can be expressed as:

$$P_{PV}(t)=n_{PV}P_{PV\_rated}\eta_{PV}\eta_{Wire}\frac{G(t)}{G_{nom}}(1-\beta_T(T_C(t)-T_{nom})) \tag{1}$$

where n_{PV} is the number PV modules, P_{PV_rated} is the rated power of the PV module at standard operating conditions (G_{nom} = 1000W/m^2 and T_{nom} = 25°C), η_{PV} is conversion efficiency of the PV module, and η_{wire} is the wiring efficiency. While G(t) is the ambient solar radiation intensity, G_{nom} is the intensity of solar radiation under standard conditions, β_T is the temperature coefficient of power of the selected PV module, $T_C(t)$ is the cell temperature, and T_{nom} is the cell temperature under standard conditions of operation. The temperature of the solar cell can be calculated in terms of the ambient temperature as follows:

$$T_C(t)-T_{ambient}=G(t)\frac{T_{Test}}{800} \tag{2}$$

where $T_{ambient}$ and T_{Test} are the ambient temperature and the temperature observed during the testing of the modules, respectively.

B. MODELLING OF THE WIND POWER SYSTEM

Starting from the fact that the wind speed changes with height, the wind speed at the desired hub height as a function of the wind speed measured at the anemometer height is given as:

$$\frac{u_2}{u_1}=\left(\frac{h_2}{h_1}\right)^{\alpha_{WT}} \tag{3}$$

where u_2 is the wind speed at the wind turbine hub with height, h_2, u_1 is the wind speed at the reference point (anemometer height), h_1 and α_{WT} is the friction coefficient, respectively. According to the recommendations of IEC standards [29], the value of the coefficient of friction is taken as 0.11 for extreme wind conditions, while 0.20 for normal wind conditions. Depending on the fundamentals of wind energy, the expected energy supplied by a wind turbine can be described as follows:

$$P_{WT}=\begin{cases}0, & u(t)<u_{cut-in}\\ \dfrac{n_{WT}\eta_{WT}P_{R\_WT}\left(u^2(t)-u_{cut-in}^2\right)}{\left(u_{rated}^2-u_{cut-in}^2\right)}, & u_{cut-in}<u(t)<u_{rated}\\ n_{WT}\eta_{WT}P_{R\_WT}, & u_{rated}<u(t)<u_{cut-off}\\ 0, & u(t)>u_{cut-off}\end{cases} \tag{4}$$

where P_{WT} is the actual power generated from the wind turbine, P_{R_WT} is the wind turbine rated power, n_{WT} is the number of wind turbines, η_{WT} is the efficiency of the wind system. Whereas $u(t)$ is the wind speed at time t, u_{cut-in} is the cut-in wind speed, at which the turbine starts to operate and generate power, u_{rated} is the wind speed at rated power, and u_{cut_off} is the cut-off wind speed, after which the wind turbine must be shut down for safety reasons.

C. BATTERY STORAGE SYSTEM

Due to the irregular nature of wind speed and solar radiation, the energy storage system is very necessary to keep a constant flow of power to the desired load. The lead-acid battery is the proposed type of battery banks in this study. The size of the battery storage system is influenced by some parameters such as battery life, ambient temperature, the capacity of the battery bank, and the depth of discharge (DOD) [17], [18]. The capacity limit of the battery system is usually assessed by the state of charge (SOC). The SOC of the storage battery system can be acquired by continuous observation of the charging and discharging energy of the battery banks. The battery state of charge at any time is calculated as follows:

- During charging mode,

$$E_{CH}(t)=\left(\frac{P_{WT}(t)-P_{load}(t)}{\eta_{conv}}+P_{PV}(t)\right)\times\Delta t\times\eta_{CH} \tag{5}$$

$$SOC(t)=SOC(t-1)(1-\sigma)+E_{CH}(t). \tag{6}$$

- During discharging mode,

$$E_{DIS}(t) = \left(\frac{P_{load}(t) - P_{WT}(t)}{\eta_{conv}} - P_{PV}(t)\right) \times \Delta t \times \eta_{DIS} \quad (7)$$

$$SOC(t) = SOC(t-1)(1-\sigma) - E_{DIS}(t). \quad (8)$$

where $SOC(t)$, $SOC(t-1)$, σ, $E_{CH}(t)$, $E_{DIS}(t)$, $P_{load}(t)$, η_{conv}, η_{CH}, and η_{DIS} are the state of charge of the battery system at time t, $(t-1)$, self-discharge rate, charging energy, discharging energy, load demand for energy at the time t, converter efficiency, the charging efficiency of the battery, and the discharge efficiency battery storage system, respectively.

D. DIESEL GENERATOR SYSTEM

Diesel generator (DG) is a conventional energy source, which is used in the hybrid renewable power system as a backup. It mainly operates when there is a deficit from the PV and wind systems and leading to failure to satisfy the demand for energy, and at the same time, the battery bank is depleted. The hourly fuel consumption for the DG, $D_f\ (t)$, can be obtained by [30]:

$$D_f(t) = \alpha_{DG} \times P_{DG}(t) + \beta_{DG} \times P_{DG\_R} \quad (9)$$

where $P_{DG}\ (t)$, P_{DG_R}, and α_{DG} & β_{DG} are the average power output of the DG per hour, rated power of the DG, and the coefficients of the fuel consumption curve of the DG. In this work, the values of these coefficients are set to 0.246 and 0.08145 for α_{DG} and β_{DG}, respectively [31].

IV. ENERGY MANAGEMENT STRATEGY

When the hybrid microgrid system is working in an isolated mode (i.e, when the power generated from the PV and wind energy systems is less than the demand for energy by the load), the battery will be in the discharge mode and the flow of power can be given as

$$P_{load}(t) \times \Delta t = P_{WT}(t) \times \Delta t + (P_{PV}(t) \times \Delta t + E_{DIS}(t)) \times \eta_{conv} \quad (10)$$

If the PV/wind with battery storage cannot satisfy the demand for energy, the shortage in power will be covered from a diesel generator. The sharing of the diesel generator can be calculated from

$$P_{DG}(t) \times \Delta t = (P_{load}(t) - P_{WT}(t)) \times \Delta t - (P_{PV}(t) \times \Delta t + E_{DIS}(t)) \times \eta_{conv} \quad (11)$$

If the power supplied by the PV and wind energy system is greater than the demand, the battery will be charged by the excess power and the flow of power can be expressed as

$$P_{load}(t) \times \Delta t = P_{WT}(t) \times \Delta t + (P_{PV}(t) \times \Delta t - E_{CH}(t)) \times \eta_{conv} \quad (12)$$

When the battery reaches its maximum charging level, the power supplied by the PV and wind turbines will be dumped. The power absorbed by the dummy load, in this case, is presented as

$$P_{dummy}(t) \times \Delta t = (P_{WT}(t) - P_{load}(t)) \times \Delta t + (P_{PV}(t) \times \Delta t - E_{CH}(t)) \times \eta_{conv} \quad (13)$$

A flowchart describing the operation of the proposed isolated hybrid microgrid system is given in Fig. 2.

V. OPTIMAL SIZING OF THE HYBRID MICROGRID SYSTEM

In this section, formulation of the optimization problem, including a novel objective function and the optimization constraints will be provided in the following sections.

A. EVALUATION PARAMETERS OF THE PROPOSED OPTIMIZATION STRATEGY

In this study, the parameters of the cost of energy (COE) and loss of power supply probability (LPSP) are considered as objective functions to be optimized, as the goal from this work is to optimize the size of a hybrid microgrid system which guarantees the reliability of the proposed energy system at the lowest possible cost.

1) COST OF ENERGY (COE)

The Net Present Cost (NPC) has been used for calculating the total cost of the hybrid microgrid. The annual cost of investment C_{ann_tot} of the system is considered as:

$$C_{ann\_tot} = C_{ann\_cap} + C_{ann\_rep} + C_{ann\_O} + C_{ann\_M} \quad (14)$$

where C_{ann_cap}, C_{ann_rep}, C_{ann_O}, and C_{ann_M} are the annual capital cost of the system components, the annual cost for replacements of the system components, annual operating cost, and annual cost for maintenance, respectively.

a: THE ANNUAL CAPITAL COST OF THE MICROGRID SYSTEM

The capital recovery factor (CRF) is used to convert the initial investment cost to annual capital cost.

$$CRF(r, n) = \frac{r(1+r)^n}{(1+r)^n - 1} \quad (15)$$

where r is the rate of interest (%) and n is the life span of the studied project.

The annual capital cost of the individual sub-systems can be calculated from the following equations:

$$\begin{cases} C_{ann\_cap\_PV} = C_{cap\_PV} \times CRF(r, M_{PV}) \\ C_{ann\_cap\_WT} = C_{cap\_WT} \times CRF(r, M_{WT}) \\ C_{ann\_cap\_batt} = C_{cap\_batt} \times CRF(r, M_{batt}) \\ C_{ann\_cap\_DG} = C_{cap\_DG} \times CRF(r, M_{DG}) \\ C_{ann\_cap\_conv} = C_{cap\_conv} \times CRF(r, M_{conv}) \end{cases} \quad (16)$$

where C_{cap_PV}, C_{cap_wind}, C_{cap_batt}, C_{cap_DG}, and C_{cap_conv} are the initial capital cost of installation of the PV system, wind system, battery bank, diesel generator, and converter, respectively. Whereas, M_{PV}, M_{wind}, M_{batt}, M_{DG}, and M_{conv}

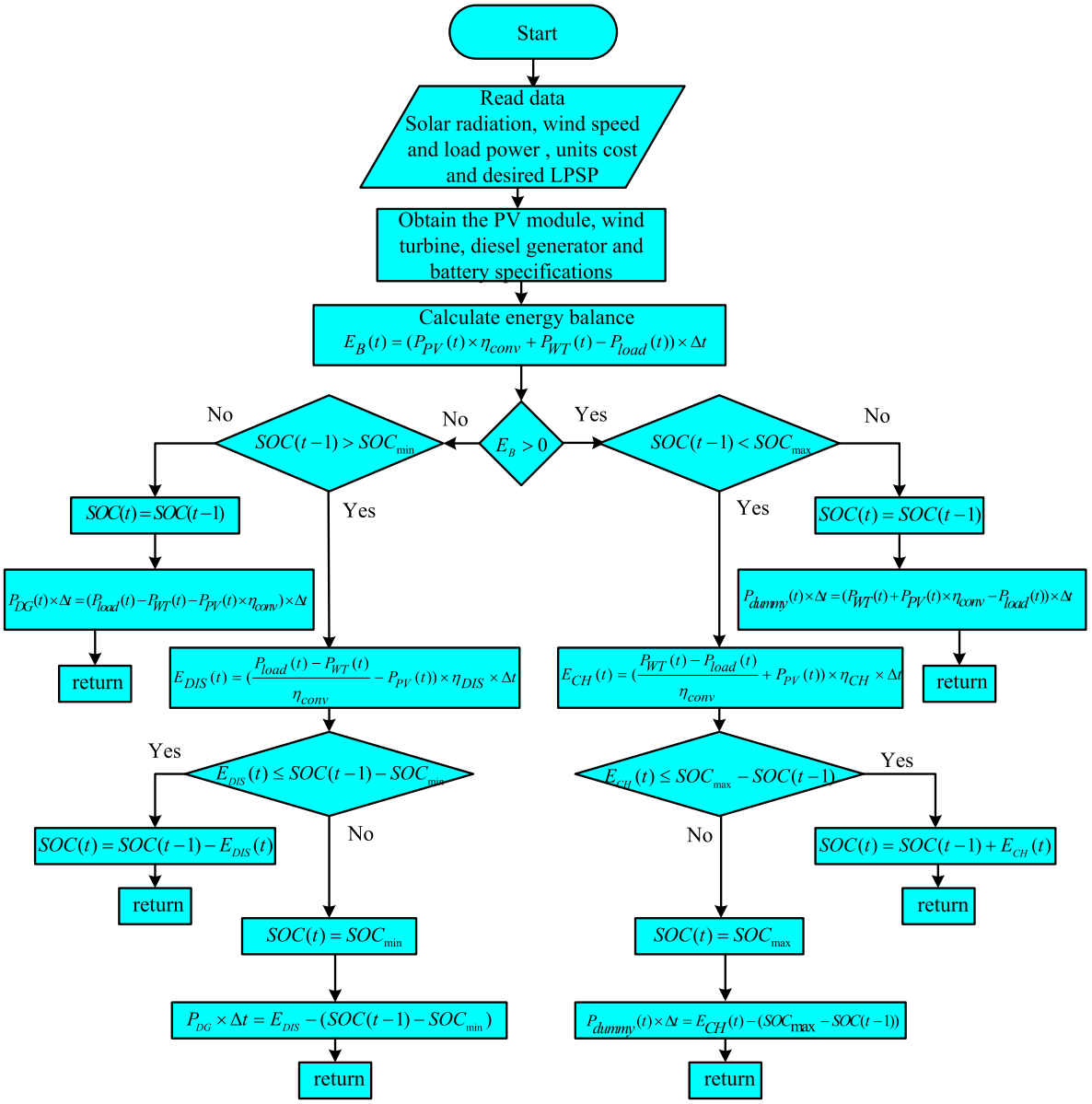

FIGURE 2. Flowchart of the proposed isolated hybrid microgrid system.

are the lifetime of PV modules, wind turbines, battery banks, diesel generator, and the converter, respectively.

Then the annual capital investment cost of the hybrid system is given as

$$C_{ann\_cap} = C_{ann\_cap\_PV} + C_{ann\_cap\_WT} + C_{ann\_cap\_batt} + C_{ann\_cap\_conv} + C_{ann\_cap\_DG} \quad (17)$$

where $C_{ann\_cap\_PV}$, $C_{ann\_cap\_wind}$, $C_{ann\_cap\_batt}$, $C_{ann\_cap\_DG}$, and $C_{ann\_cap\_conv}$ are the annual share of the capital cost of installation of the PV system, wind system, the battery bank, the diesel generator, and converter, respectively.

b: THE OPERATING AND MAINTENANCE COST

The operating and maintenance cost of the system is defined as

$$C_{O\&M} = C_{O\&M\_PV} \times t_{PV} + C_{O\&M\_WT} \times t_{WT} + C_{O\&M\_batt} \times t_{batt} + C_{O\&M\_conv} \times t_{conv} + C_{O\&M\_DG} \times t_{DG} \quad (18)$$

where $C_{O\&M\_PV}$, $C_{O\&M\_WT}$, $C_{O\&M\_batt}$, $C_{O\&M\_conv}$, and $C_{O\&M\_DG}$ are the operating and maintenance cost of PV, wind turbine, battery banks, converter, and diesel generator per unit time, respectively. While, t_{PV}, t_{WT}, t_{batt}, t_{conv}, and t_{DG} are the

operating time of PV, wind turbine, battery banks, converter, and diesel generator, respectively.

c: THE ANNUAL REPLACEMENT COST

The present value of the replacement cost of the hybrid system components within the system lifetime can be calculated from the following equation [32]:

$$C_{rep} = \sum_{j=}^{n_{rep}} \mathrm{K}_{C\_rep} \mathrm{C}_u \left(\frac{1+i}{1+r}\right)^{nj/(n_{rep}+1)} \tag{19}$$

where i, K_{C_rep}, C_u and n_{rep} are the inflation rate of replacement, the capacity of the units used in the system, the cost of the replaced units, and the number of replacements over the project lifetime n, respectively.

The net present cost (NPC) of the system can be calculated by

$$NPC = \frac{C_{ann\_tot}}{CRF} \tag{20}$$

The cost of energy (COE) is the cost of the generated electrical energy from the hybrid system in ($/kWh) and formulated in the following equation:

$$COE = \frac{C_{ann\_tot}}{\sum_{h=1}^{h=8760} P_{load}} = \frac{NPC}{\sum_{h=1}^{h=8760} P_{load}} \times CRF \tag{21}$$

2) LOSS OF POWER SUPPLY PROBABILITY

The loss of power supply probability (LPSP) is a design factor, which measures the probability of insufficient operation of the power supply when the hybrid microgrid, in our case study, fails to satisfy the demand for energy. This case occurred when the sum of the total power generated is less than the load power. The loss of power supply at any period of time $LPS(t)$ can be defined as:

$$\begin{aligned} LPS(t) &= P_{Load}(t) \times \Delta t \\ &- (P_{DG}(t) + P_{WT}(t)) \times \Delta t \\ &- ((P_{PV}(t) \times \Delta t) + SOC(t - \Delta t) - SOC_{\min}) \times \eta_{conv} \end{aligned} \tag{22}$$

LPSP is very common among researchers as a technical index for evaluating the reliability in the problems of optimal sizing of hybrid renewable energy systems. The value of LPSP can be formulated mathematically as the sum of all the observed values of $LPS(t)$ over the all load demand for energy during the entire period of study.

$$LPSP = \frac{\sum_{t=1}^{8760} LPS(t)}{\sum_{t=1}^{8760} P_{load}(t) \times \Delta t} \tag{23}$$

Moreover, during the analysis of system reliability, the following condition is added

$$P_{load}(t) > P_{tot\_generation}(t) \tag{24}$$

B. OBJECTIVE FUNCTION

In this work, the proposed objective function of the optimization algorithms is in terms of the cost of energy (COE), loss of power supply probability (LPSP), and the dummy load (P_{dummy}). This function can be expressed as

$$\min_x f = \min_x (\lambda_1 COE + \lambda_2 LPSP + \lambda_3 P_{dummy}) \tag{25}$$

where, x is a four-dimensional vector consisting of the optimization parameters ((i) number of PV modules n_{PV}, (ii) number of wind turbines n_{WT}, (iii) number of battery storage banks n_{Batt}, and (iv) number of diesel generators n_{DG}). λ_1, λ_2, and λ_3 are chosen via trial and error method, in order to achieve the best results. In this work, the values of λ_1, λ_2, and λ_3 are set to 0.4, 0.599 and 0.001, respectively.

C. DESIGN CONSTRAINTS FOR OPTIMIZATION

In off-grid hybrid systems, the components of the power system are operating under constraints. The optimal operation of the system should fulfill the constraint function described in Eq. (26), which means that the power is balanced at any time. The optimization strategy used to ensure that the hourly power supplied by DG at any time must be less than or equal to the DG rated power as defined by Eq. (27). In order to avoid the overcharging and undercharging problems, the SOC of the battery bank is constrained and compared with the designed constraints at any hour during the operation period. Therefore, the SOC of the battery storage system should satisfy the design constraints presented in Eqs. (28) and (29). The maximum state of charge SOC_{max} is the full capacity of the battery bank, while the minimum state of charge SOC_{min} depends mainly on the depth of discharge. In addition, the LPSP should less than the predefined reliability index (β_L) of the system as expressed in formula Eq. (30) and, in this study, β_L is considered to be less than 0.04.

$$P_{PV}(t) + P_{WT}(t) + P_{DG}(t) + P_{batt}(t) = P_{load}(t) \tag{26}$$

$$P_{DG}(t) \leq P_{DG\_rated} \tag{27}$$

$$SOC_{\min} \leq \mathrm{SOC}(t) \leq SOC_{\max} \tag{28}$$

$$\mathrm{SOC}(t+1) = SOC(t)(1-\sigma) \tag{29}$$

$$LPSP \leq \beta_L \tag{30}$$

VI. OPTIMIZATION TECHNIQUES

In this section, a clear discussion and analysis of the proposed optimization techniques, which are WOA, WCA, MFO, and PSOGSA have been provided.

A. WHALE OPTIMIZATION ALGORITHM

Whale Optimization Algorithm (WOA) was firstly suggested in the work of Mirjalili and Lewis in 2016 [33]. Humpback whale is one of the huge baleen whales. WOA has been established according to the hunting technique, which is called bubble-net feeding technique. This type of whales

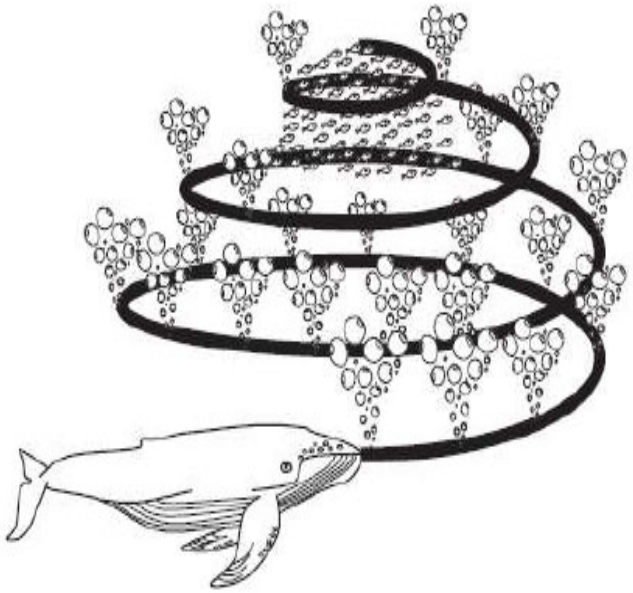

FIGURE 3. Bubble-net feeding mechanism.

chases and hunts their preys near the surface of the water by making a special stream of bubbles of spiral shape as illustrated in Fig. 3. The mathematical representation of WOA is explained in this section.

1) SURROUNDING THE PREY

As the place of the optimal solution in the search space is not defined, the WOA assume that the best objective prey is the candidate solution. As a result, the other search agents change their site in accordance with the predetermined best agent position [33].

$$\vec{D} = \left|\vec{C}.\vec{X}^*(t) - \vec{X}(t)\right| \tag{31}$$

$$\vec{X}(t+1) = \vec{X}^*(t) - \vec{A}.\vec{D} \tag{32}$$

where t refers to the present iteration, $\vec{A}$ and $\vec{C}$ defined as coefficient vectors, $\vec{X}^*$ is a vector describes the location of the best value, and $\vec{X}$ is a vector describes the position of the whale. $\vec{A}$ and $\vec{C}$ vectors are calculated from

$$\begin{aligned} \vec{A} &= 2\vec{a}.\vec{r}_1 - \vec{a} \\ \vec{C} &= 2.\vec{r}_2 \end{aligned} \tag{33}$$

where $\vec{a}$ refers to the components of each vector, which decreased from 2 to 0 in each iteration, $\vec{r}_1$ and $\vec{r}_2$ are taken as random vectors in [0, 1].

2) BUBBLE NET ATTACKING TECHNIQUE (EXPLOITATION PHASE)

Two approaches are prepared for the Bubble-net behavior technique of the Humpback whales:

- Shrinking encircling mechanism: by minimizing the value of $\vec{a}$ in Eq. (33), this technique will be obtained. Accordingly, the updated position of the search agent could be evaluated by the first position and the obtained best location in the present iteration.
- Spiral updating position: Humpback whales dive down and produce a stream of bubbles in a spiral shape around its goal (prey). In this approach the distance separating the whale from its prey is firstly computed, then a spiral equation between the location of the prey and the whale, which takes the spiral shape, is mathematically explained in Eq. (34).

$$\vec{X}(t+1) = \vec{D}'.e^{bl}.\cos(2\pi l) + \vec{X}^*(t) \tag{34}$$

where, $\vec{D}' = \left|\vec{X}^*(t) - \vec{X}(t)\right|$, b is a constant number for determining the shape the spiral, and l is a random number between $[-1, 1]$ as given in [34]. Humpback whales swim around the prey inside a shrinking range and over a helix-shaped way simultaneously. Then, two probabilities are considered to choose between them and can be mathematically modeled in the following formula:

$$\vec{X}(t+1) = \begin{cases} \vec{X}^*(t) - \vec{A}.\vec{D}, & if\ -p < 0.5 \\ \vec{D}'.e^{bl}.\cos(2\pi l) + \vec{X}^*(t), & if\ -p \geq 0.5 \end{cases} \tag{35}$$

where p is a random number in [0, 1].

3) SCAN FOR PREY (INVESTIGATION STAGE)

Besides the bubble-net mechanism, the Humpback whales search for hunting the prey arbitrarily in the iteration. The mathematical model is expressed in the following:

$$\vec{D} = \left|\vec{C}.\vec{X}_{rand} - \vec{X}(t)\right| \tag{36}$$

$$\vec{X}(t+1) = \vec{X}_{rand} - \vec{A}.\vec{D} \tag{37}$$

The flowchart describing the operation of WOA is shown in Fig. 4.

B. WATER CYCLE ALGORITHM (WCA)

Water cycle algorithm (WCA) is a developed meta-heuristic optimization technique, which is a part of the evolutionary algorithms. The idea of the proposed WCA is inspired by nature and based on the watershed control process describing how rivers and streams flow into the sea. When it rains, the raindrops combine to form a flow of water, and the weak flow merged to create a powerful water current that systematically accumulates into a stream and runs towards the sea. In this cycle, some water leaks to the ground, some of which flow through the surface of the earth, some evaporate and form rain creating new water droplets and streams, extending the distinction of the population.

Comparable to other metaheuristic algorithms, the WCA optimization method begins with a random initial population, which termed the population of streams. First of all, rain or precipitation is assumed. Then, the best stream is selected to be the sea. After that, the good streams (N_{sr}) following the best one (sea) are selected as rivers [35], [36]. Moreover, N_{sr} represents the combination of rivers and sea.

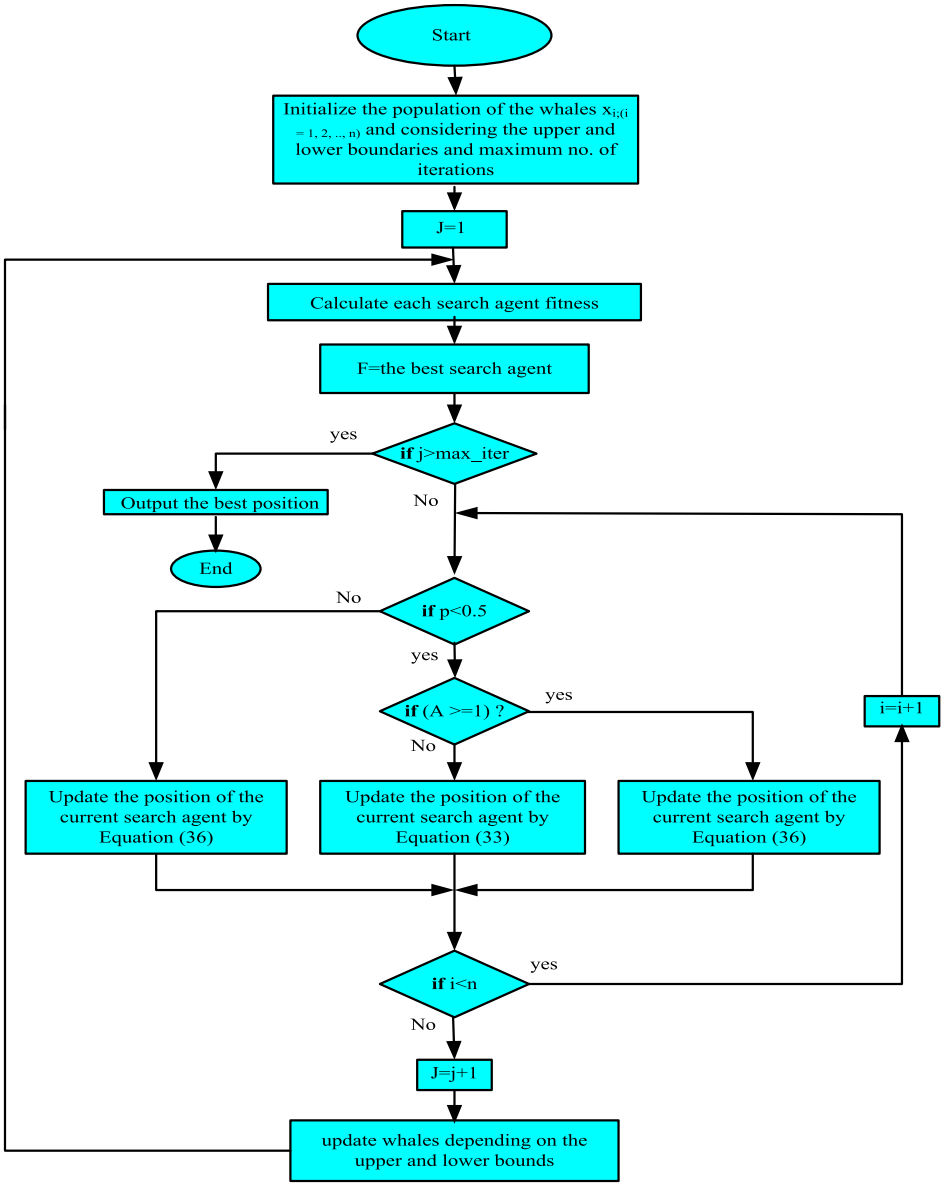

FIGURE 4. Flowchart of WOA optimization technique.

Taking into account the quantity of water flow, which represents the fitness/cost function, rivers and sea soak up these streams. By nature, streams run towards rivers and rivers in turn towards the sea, but some of these streams by a direct route flow towards the sea (Eq.38). The new positions of the streams and rivers have been updated according to the following [35]:

$$\vec{X}^i_{stream}(t+1) = \vec{X}^i_{stream}(t) + rand \times C \times \left(\vec{X}^i_{sea}(t) - \vec{X}^i_{stream}(t)\right) \quad (38)$$

$$\vec{X}^i_{stream}(t+1) = \vec{X}^i_{stream}(t) + rand \times C \times \left(\vec{X}^i_{river}(t) - \vec{X}^i_{stream}(t)\right) \quad (39)$$

$$\vec{X}^i_{river}(t+1) = \vec{X}^i_{river}(t) + rand \times C \times \left(\vec{X}^i_{sea}(t) - \vec{X}^i_{river}(t)\right) \quad (40)$$

where, *rand* is an arbitrarily number distributed uniformly between [0, 1], while C between [1, 2].

For the exploration stage, when the distances among streams, rivers, and sea are less than the predefined maximum value (*dmax*), new streams are produced towards the rivers and sea (i.e., evaporation state). Figure 5 demonstrates the schematic diagram for WCA, in which circles correspond to the streams, stars to rivers, and the diamond to sea. The flowchart of the WCA optimization algorithm is shown in Fig. 6.

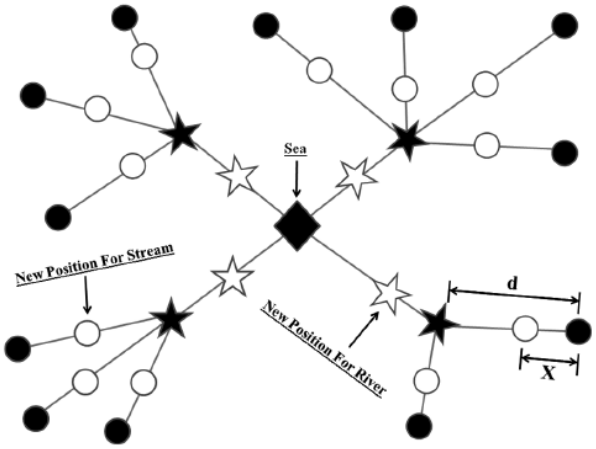

FIGURE 5. Schematic representation of the movement of WCA towards the optimal solution.

C. HYBRID PSOGSA OPTIMIZATION ALGORITHM

The particle swarm optimization (PSO), developed in 1995 by Kennedy and Eberhart, is a population-based meta-heuristic technique, whose concept is inspired by the flocking manner of the birds [37], [38]. In this technique, a number of particles are used as candidate solutions flying in the search space to form a population searching for the global optimal solution. Through their paths, the position of each particle is barred by its best position, the personal best (p_{best}) and the global best (g_{best}). For each particle, the present location in the search space is represented by the current speed, and the distance to the personal best and global best are used to modify the position and speed of each particle, which is mathematically modeled as following [39]:

$$v_i(n+1) = w \times v_i(n) + c_1 \times rand \times (pbest - x_i(n)) + c_2 \times rand \times (gbest - x_i(n)) \quad (41)$$

$$x_i(n+1) = x_i(n) + v_i(n+1) \quad (42)$$

In the above equation, $v_i(n)$ is the speed of "i^{th}" particle in the iteration "n", w is the inertia weight, which is initially introduced in the algorithm. *rand* is a random number between [0, 1]. $x_i(n)$ represents the present position of the "i^{th}" particle in the "n^{th}" iteration. "c_1" and "c_2" are positive constants, which refer to the weighting factors responsible for changing the velocity of each particle towards p_{best} and g_{best}. Eq. (42) is used for updating the position of the particle, taking into account the position and speed in the previous iteration. Eq. (41) consists of three sections, the first section $w \times v_i(n)$ represents the PSO exploration ability. The second $c_1 \times rand \times (pbest - x_i(n))$ and third section $c_2 \times rand \times (gbest - x_i(n))$ introduces the private thinking and coaction of particles [39]. In each iteration, Eq. (41) is used for calculating the speed of the particles then Eq. (42) used for updating the positions of the particles. The process is continued until the target of the PSO is reached.

The gravitational search algorithm (GSA), implemented by E. Rashedi *et al.* in 2009, is a novel meta-heuristic optimization technique, whose concept is based on the laws of gravity and interaction of masses developed by Newton [37], [38], [40]. The theory says "there is a force of attraction between each particle and other particles in its surrounding universe, which is directly proportional to the product of the masses of subjected particles and inversely with the square of the spacing between these particles"

In GSA during the evaluation process, the objects are taken as agents (elected solutions), where their performance is evaluated by their masses, which are proportional to the fitness function. In this process, all objects attracted to each other. In addition, the heavy masses have higher forces of attraction. Therefore, they have a highest fitness function and taken as a best optimal solution. Moreover, the heaviest mass moves in the search space slower than other worse solutions.

In GSA the mass of each object is characterized by four indicators; the position of the mass X_i, the mass of inertia M_{ii}, the active gravitational mass M_{ai}, and finally the passive gravitational mass M_{ip}.

At the initialization stage of the algorithm, a population of N masses, which is considered as candidate solution, is considered and the position of each mass in the search space is described as follows:

$$X_i = \left(x_i^1, \ldots, x_i^d, \ldots x_i^n\right), \quad i = 1, 2, \ldots\ldots N \quad (43)$$

According to the gravitational law of Newton, the gravitational force that mass j makes towards the mass i at any time t is given as [40]:

$$F_{ij}^d(t) = G(t)\frac{M_{pi}(t) \times M_{aj}(t)}{R_{ij}(t) + \varepsilon}(x_j^d(t) - x_i^d(t)) \quad (44)$$

where $G(t)$ is gravitational constant at a specified time "t", ε is a small constant, $R_{ij}(t)$ is Euclidean spacing between the two candidates i and j, M_{aj} is the active gravitational mass, M_{pi} is passive gravitational mass. The gravitational constant G is evaluated as:

$$G(t) = G_o \times \exp(-\alpha \times iter / \max itere) \quad (45)$$

where G_O is the initial value of gravitational constant, α is a descending coefficient, *iter* is present iteration, and "*max-itere*" is the maximum iterations number. The total force influencing the agent i is explained as follows:

$$F_i^d(t) = \sum_{j=1, j\neq i}^{N}(rand_j)(F_{ij}^d(t)) \quad (46)$$

where, $rand_j$ is a random number ranges between [0, 1]. According to the law of motion, the accelerations of all agents are given as follows:

$$ac_i^d(t) = \frac{F_i^d(t)}{M_i(t)} \quad (47)$$

where M_i is the mass of the candidate solution "i", "t" is the current iteration, and "d" is the optimization problem dimension.

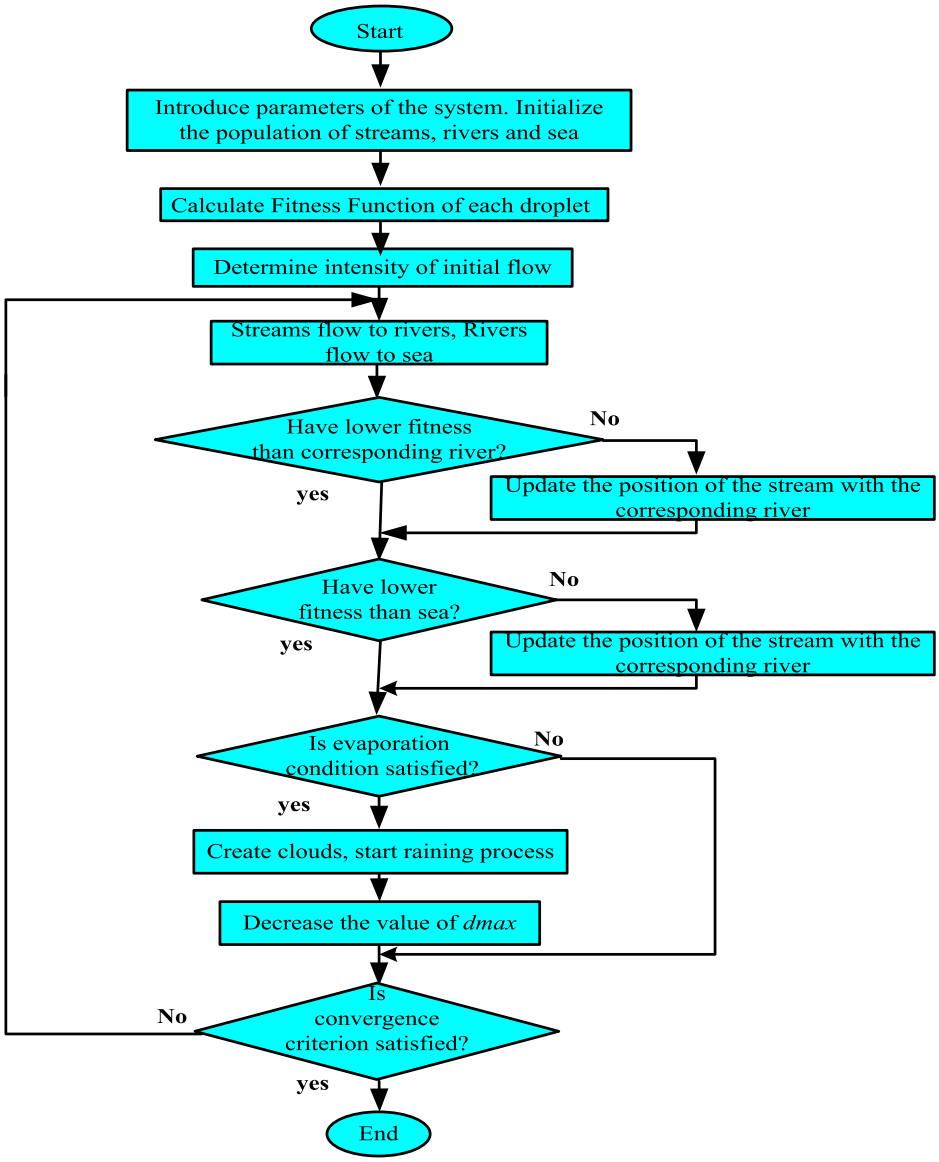

FIGURE 6. The flowchart of the WCA optimization technique.

For each iteration, the velocity and position of agents in each population are computed from the following:

$$v_i^d(t+1) = rand_i \times v_i^d(t) + ac_i^d(t) \quad (48)$$

$$x_i^d(t+1) = x_i^d(t) + v_i^d(t+1) \quad (49)$$

where x_i^d is the position of agent i, x_i^d is the velocity of agent i at the iteration "t", and d is the dimension of the optimization problem. From the above equations, the present velocity of the search agent equals a fraction between [0, 1] added to its final acceleration. The current position of the search agent equals to its final position added to the present velocity.

GSA is characterized by two important merits: (i) the capability of the technique to seek the entire search area "exploration", which can be implemented by proper selection of G_o and α, and (ii) the ability to deed the optimal solution "exploitation", which is guaranteed by slow movement of heavy masses. According to the last equations from Eqs. (45) to (49), the operation process of GSA is continued until reaching the end criterion.

To avoid the weakness of both techniques, particle swarm optimization and gravitational search algorithm are hybridized in parallel forming a new population-based meta-heuristic optimization algorithm called PSOGSA [37].

The main advantage of PSOGSA is to merge the high efficiency of exploitation in PSO with the good exploration capability of GSA. The velocity and position of the search agents according to the combination of the two algorithms

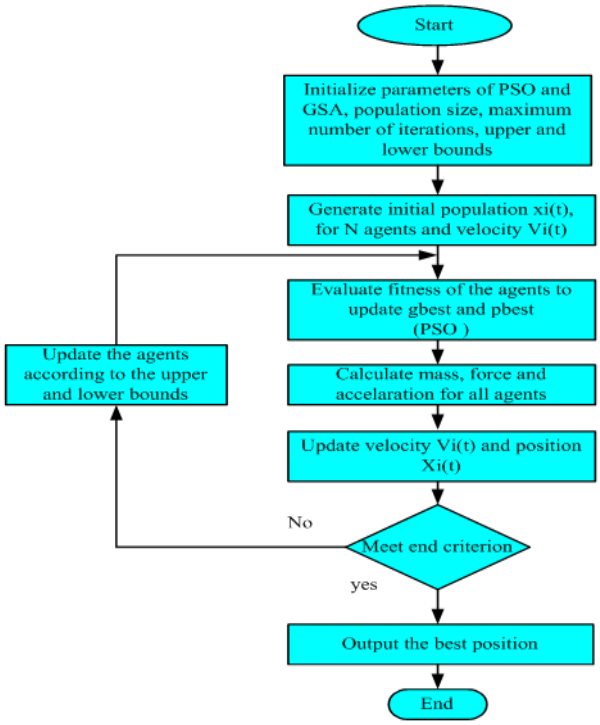

FIGURE 7. The flowchart of PSOGSA algorithm.

are calculated from the following:

$$V_i(n+1) = w \times V_i(n) + c_1^{'} \times rand \times ac_i(n) + c_2^{'} \times rand \times (gbest - X_i(n)) \quad (50)$$

$$X_i(n+1) = X_i(n) + V_i(n+1) \quad (51)$$

where $V_i(n)$ is the velocity of the search agent i, $c_1^{'}$ and $c_2^{'}$ is the acceleration coefficients, w is defined as a weight factor.

In this study, in PSOGSA meta-heuristic optimization algorithm, the candidate solutions are taken as the agents of a randomly generated population. After initialization according to the procedure of GSA, the gravitational constant is computed, then the fitness function of all search agents is estimated. Then the force, the gravitational constant, the values of agent mass, and gravitational acceleration; have been estimated based on Eqs. (44) to (47). Then according to Eq. (50), the velocity of each search agent is calculated depending on the present acceleration and the best position. Finally, using Eq. (51), the position of all particles in the search space is updated. So, in each iteration, the best solution (g_{best}) and (p_{best}) for all objects are changed. The above procedure is repeated until the proposed system reaches the end criterion. The procedure of the hybrid PSOGSA optimization algorithm is summarized in the flowchart shown in Fig. 7.

D. MOTH-FLAME OPTIMIZER

Moth-flame optimizer (MFO) is a novel developed optimization technique, firstly implemented by Mirjalili in 2015 [41]. In the MFO optimization method, moths are assumed to be the elected solutions, while the variables of the optimization problem are taken as the position of these candidates in the search area. According to this, moths can fly in different areas (1-dimensional, 2-dimensional, 3-dimensional or hyper-dimensional) by updating their position vector. As the MFO is a population-based algorithm, the following matrix introduces the set of generated moths [41], [42],

$$M = \begin{pmatrix} m_{11} & m_{12} & \dots & m_{1d} \\ m_{21} & m_{22} & \dots & m_{2d} \\ \dots & \dots & \dots & \dots \\ m_{n1} & m_{n2} & \dots & m_{nd} \end{pmatrix} \quad (52)$$

where n refers to the number of moths and d for the coincided design variables.

The values of the proper fitness values corresponding to all moths; can be assumed and stored as below [41], [43]:

$$OM = \begin{pmatrix} OM_1 \\ OM_2 \\ \dots \\ OM_n \end{pmatrix} \quad (53)$$

Another important component of the MFO method is the flames, which are described as similar to the way of moths [41]:

$$F = \begin{pmatrix} F_{11} & F_{12} & \dots & F_{1d} \\ F_{21} & F_{22} & \dots & F_{2d} \\ \dots & \dots & \dots & \dots \\ F_{n1} & F_{n2} & \dots & F_{nd} \end{pmatrix} \quad (54)$$

In addition, it is assumed that there is a matrix for storing fitness values as:

$$OF = \begin{pmatrix} OF_1 \\ OF_2 \\ \dots \\ OF_n \end{pmatrix} \quad (55)$$

In the MFO, both moths and flames are considered as the solution. The moths are the actual search agents, which execute the search space, while the flames act as the best location of the moths so far. In other words, flames can be assumed as flags or pins directed by moths in the process of searching the space. Then, each moth looks for nearby a flag (flame) and changes it to detect a superior solution. With this technique, a moth possesses the best position [41].

The MFO configuration has three approximation functions; the initialization function I; the main function P; and the termination function T. The overall frame of the MFO technique can be considered as [41], [42]:

$$MFO = (I, P, T) \quad (56)$$

The initialization function I randomly generates a population of moths with their fitness values as expressed in the following

$$M(i,j) = ub(i) - lb(i) \times rand() + lb(i) \quad (57)$$

$$OM = fitnessFunction(M) \quad (58)$$

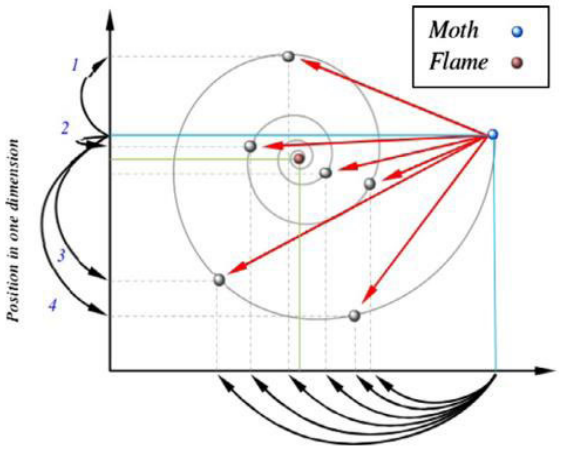

FIGURE 8. Some of the possible positions that can be reached by a moth with respect to a flame using the logarithmic spiral.

When the initialization process is finished, the P function starts operation until the termination function T is fulfilled. The logarithmic spiral function is considered as the main mechanism for updating the position of moths in accordance with their corresponding flame [43].

The following formula is used for updating the position of each moth towards the corresponding flame:

$$M_i = S(M_i, F_j) \tag{59}$$

where M_i, F_j, and S indicate the i-th moth, the j-th flame, and the spiral function, respectively. The logarithmic spiral for the MFO main update mechanism is expressed as:

$$S(M_i, F_j) = D_i.e^{bt}.\cos(2\pi t) + F_j \tag{60}$$

where D_i, b, and t are the distance of the i-th moth for the j-th flame, a constant for explaining the form of the logarithmic spiral, a random number between [1, −1], respectively. D_i is estimated from the following expression:

$$D_i = \left|F_j - M_i\right| \tag{61}$$

The spiral function is considered to make sure that a moth flies nearby a flame and not blocked in the area between them. Figure 8 shows the mechanism that the moth uses to update its positions around the flame. Exploration stage occurs if the next position of moth lies outside the search space between it and the flame. On the other hand, the exploitation process takes place when the next location lies in the area between the moth and flame. The flowchart of the MFO algorithm is shown in Fig. 9:

The following steps are used for more declaration of the MFO algorithm operation:

- Assigning each moth a flame, and then updating the location of flames in each iteration.
- To confirm that the moths never get lost in the search area between it and the corresponding flame and assuring the convergence of the MFO technique, the present best position obtained is stored as a guide for the moths in the next iteration.

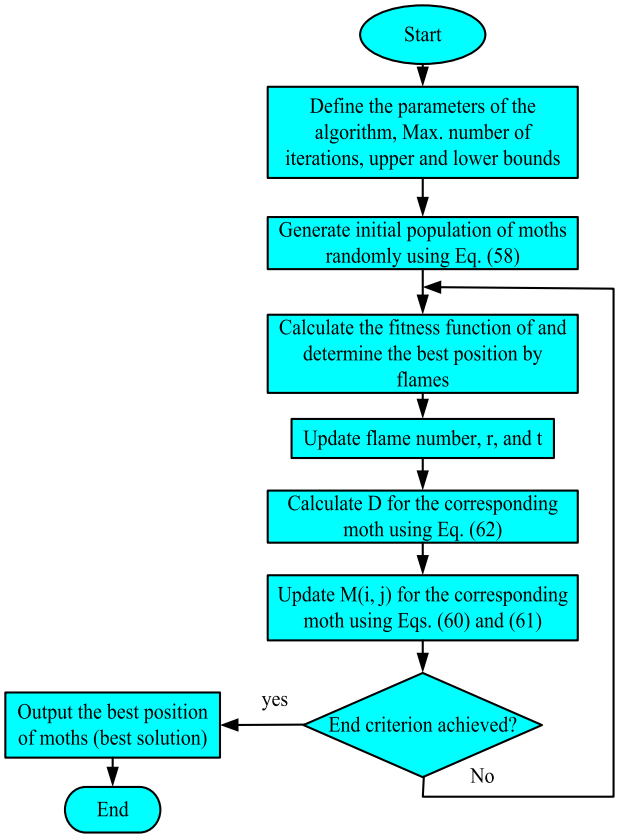

FIGURE 9. Flow chart of the MFO optimization algorithm.

- The exploration and exploitation processes are balanced according to the adaptive number of flames.
- The acceleration convergence nearby the corresponding flames over the iterations is influenced by the constant of adaptive convergence (r).

VII. THE STUDY CASE

In this study, the proposed microgrid in this study is considered for Abu-Monqar village in Farafra Oasis, New Valley governorate situated in the south-west of Egypt, in Western Desert. According to the geographical location, the village is located at latitude 26.5 N, longitude 27.7 E, and 133m above the seawater level (see Fig. 10). It is about 250 kilometers from the El-Dakhla Oasis, 450 kilometers from El-Kharga Oasis and about 100 kilometers from the administrative center of Farafra Oasis, which is about 600 kilometers away from Cairo.

It has a population of about 7 thousand people, the only region in the Arab Republic of Egypt, which did not reach the grid electricity and live on the electricity of diesel machines, which works about 14 hours a day.

The data of the intensity of solar radiation over the horizontal surface and wind speeds were obtained from, NASA depending on the long-term average of meteorological parameters of 20 years of observation. The detailed potential of the solar radiation and wind speed in the selected site

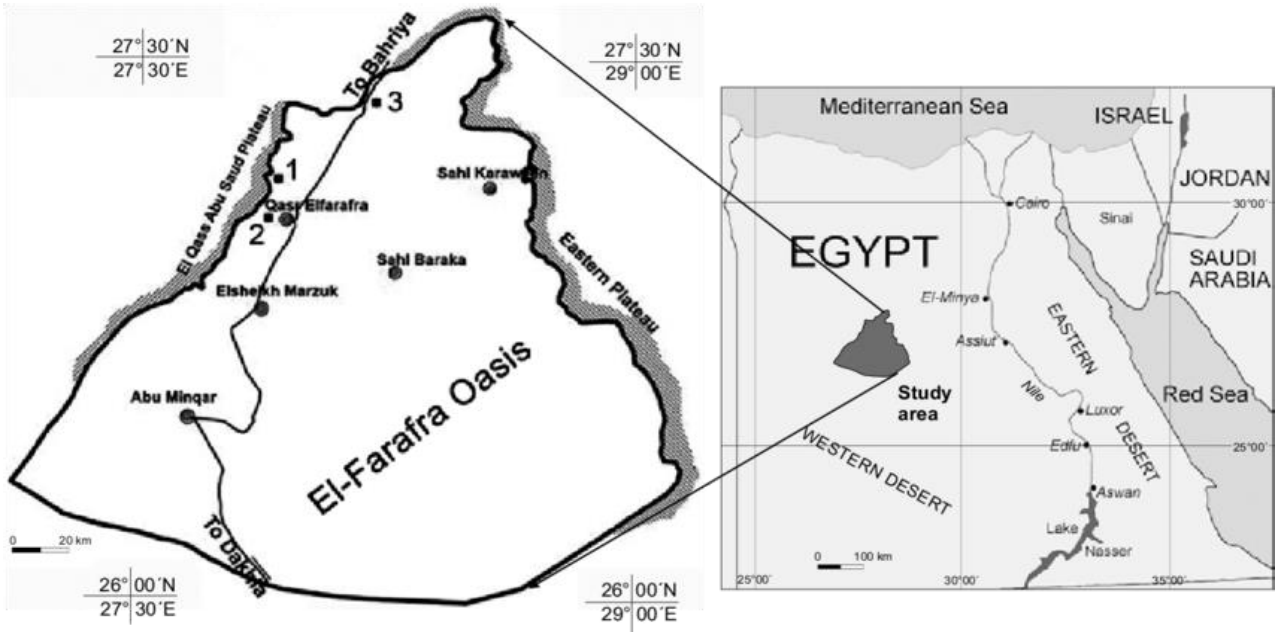

FIGURE 10. The location of the studied village, namely abu-monqar village located in the south-west of Egypt.

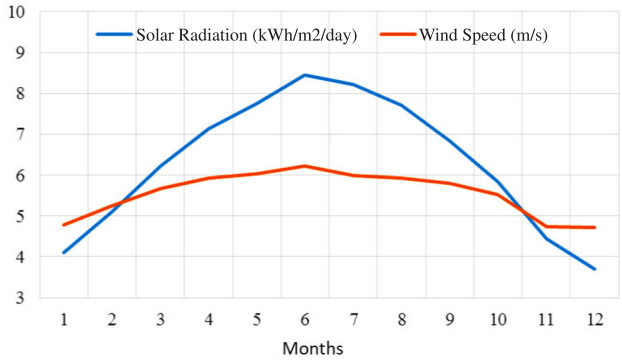

FIGURE 11. Average monthly solar radiation and wind speed for the study area.

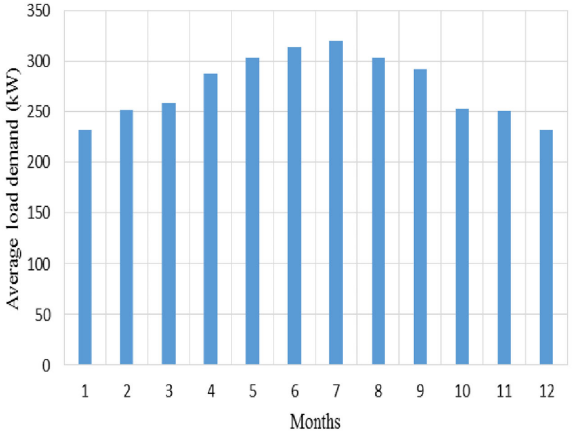

FIGURE 12. The monthly average load demand.

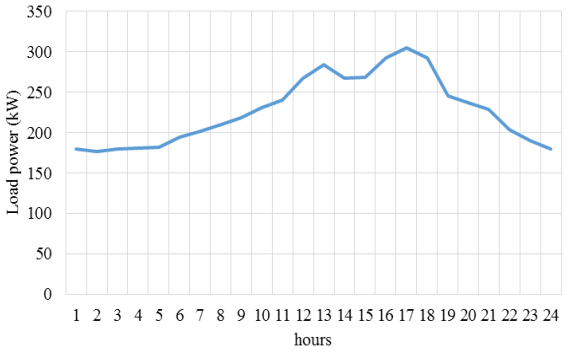

FIGURE 13. The daily load curve of the study area.

is shown in Fig. 11. The annual average radiation on the horizontal surface for this village is about 6.04 kWh/m^2/day while its annual radiation ranges between 3.64kWh/m^2/day and 8.12kWh/m^2/day. The potential of wind energy in the south of Egypt was studied in [8]. The authors concluded that the wind speed is more persistent and blow over this region with frequencies from 67% to 87% over the year in two main sectors N and NNW with average wind speed in the range of 6.8 to 7.9 m/s [8]. The main loads in this area are residential loads for lighting and other domestic facilities. Taking into account the short period of availability of electricity in the village, the maximum load observed was about 420 kW, while the average demand for electricity was 265 kW. Taking into consideration the nature of living in this region, a daily load curve has been proposed. The peak load occurs in the period from 19:00 to 22:00 o'clock as the major load of the selected area is the lighting. The monthly averaged load demand is shown in Fig. 12, while the suggested daily load curve for a certain day is presented in Fig. 13.

The main goal of the optimization techniques is to minimize the objective functions of equation (25) and determine the best optimal size of the components of the RES microgrid,

which are: (i) number of PV modules n_{PV}, (ii) number of wind turbines n_{WT}, (iii) number of battery storage banks n_{Batt}, and (iv) number of diesel generators n_{DG}. In this research, each optimization algorithm operates according to the following steps:

A. Run the program of designing the RES based on the energy balance, which has three main steps:
   1. Generation of the initial population.
   2. Run the program of designing the RES described in equations from (1) to (23), as illustrated in the flowchart presented in Fig. 2.
   3. The evaluation process of the fitness function for all agents/positions given in Eq. (25).

B. Run the optimization algorithm with the RES, which involves the following processes:
   1. Updating the position and sizing the RES elements, according to the nature of each optimization algorithm.
   2. Run the program of designing the RES described in equations from (1) to (23), as illustrated in the flowchart of Fig. 2.
   3. The evaluation process of the fitness function for all agents/positions presented in Eq. (25).
   4. Check whether the proposed system meets the end criterion or not. If so, (i.e., ''Yes''), the program will be stopped and will go to the next step, otherwise (i.e., ''No''), the three previous processes, namely from ''1'' to ''3'', will be repeated.
   5. Show the results such as sizing of RES and the best optimum values of COE, NPC, LPSP and Dummy load.

VIII. RESULTS AND DISCUSSION

A small village located in the southwest of Egypt deeply in Western Desert has been used for assessing the optimization of sizing a small-size isolated hybrid microgrid. Based on the existing data, the annual average wind speed in the selected site is about 5m/s and the average horizontal solar radiation is 6.04kWh/m^2/day.

The technical and economic specifications of PV, wind turbine, battery bank, and diesel generator, used in this study has been presented in Table 1. In the present work, the rate of interest has been taken as 6%, while the lifetime of the system has been chosen as 25 years.

The results were accomplished using MATLAB simulation program. The control parameters and the boundaries of the optimized variables are the same for the proposed optimization algorithms used in this study. The maximum number of iterations was set to 50 iterations and the maximum number of search agents is 20.

A. OPTIMAL COMBINATION OF THE SYSTEM COMPONENTS

In this study, the size of the proposed microgrid is defined as the number of PV modules, the number of wind turbines, the number of battery banks, and the number of diesel generator units.

In this study, the size of the proposed microgrid is defined by the number of (i) PV modules, (ii) wind turbines, (iii) battery banks, and (iv) diesel generator units. Table 2 shows the detailed results of the optimization process, while the optimization algorithms were evaluated considering 10 and 50 iterations. It can be seen in Fig. 14 that WOA reached the optimum solution of 0.228833 within the predefined operation limits after 23 iterations, while WCA reached the best cost of 0.229951 after 16 iterations, MFO reached the best cost of 0.2299526 after 41 iterations, and PSOGSA reached the best cost of 0.2300714 after 14 iterations.

TABLE 1. Technical and economic characteristics of the system components

Component	Parameter	Value	Unit
PV	Model	PV-MLT260HC	
	Max. power	260	Watt
	Length	1625	Mm
	Width	1019	Mm
	Thickness	46	Mm
	Module efficiency	15.7%	
	Operating temperature	47	ºC
	Temperature coefficient	0.45%	
	Initial cost	112	$
	O&M cost	1%	
	Lifetime	25	year
Wind Turbine	Model	Fuhrländer FL 30	
	Rated power	30	kW
	Rotor diameter	12.8	m
	Swept area	13	m^2
	Cut-in speed	2.5	m/s
	Rated speed	12	m/s
	Cut-off speed	25	m/s
	Initial cost	58564.79	$
	O&M cost	3	%
	Replacement cost	34553.226	$
	Lifetime	20	year
Battery Bank	Model	RS lead-acid battery	
	Size	12V(50Ah)	
	Efficiency	86	%
	DOD	0.8	
	Weight	16.5	kg
	Max. discharge current	750	A
	Internal resistance	<=0.006	Ω
	Operating temperature	0-40	ºC
	Initial cost	146.5	$
	Replacement cost	102.55	$
	Lifetime	10	Year
Diesel Generator	Rated power	100	kW
	Initial cost/kW	850	$
	Replacement cost/kW	850	$
	O&M cost	3	%
	Lifetime	10	Year

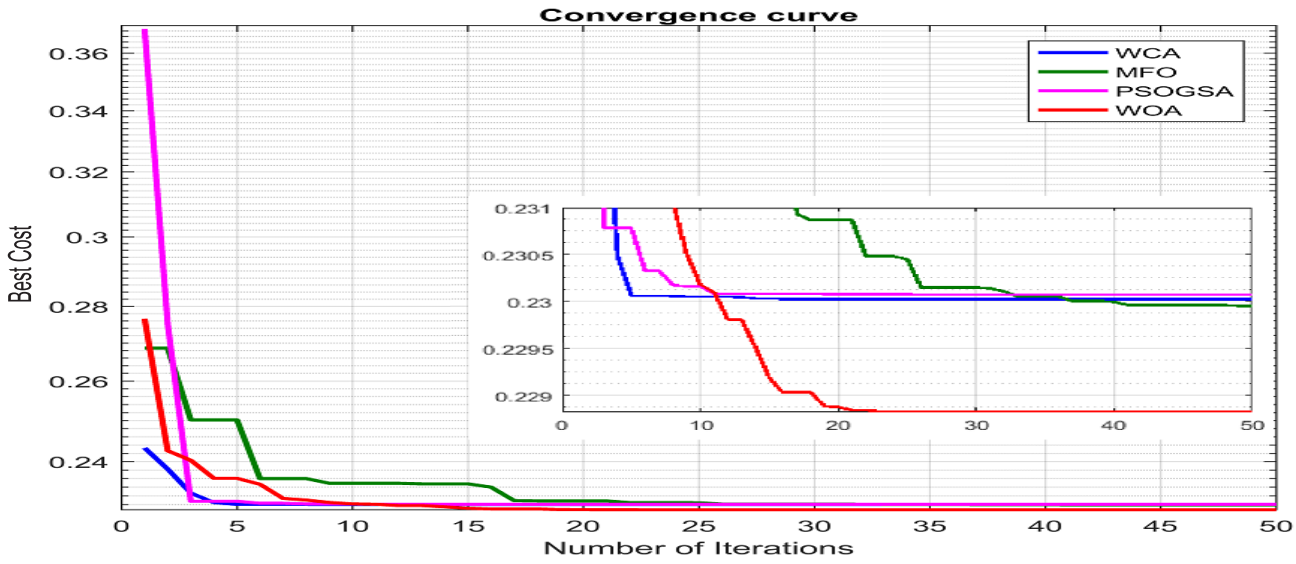

FIGURE 14. Convergence curves of the proposed optimization techniques.

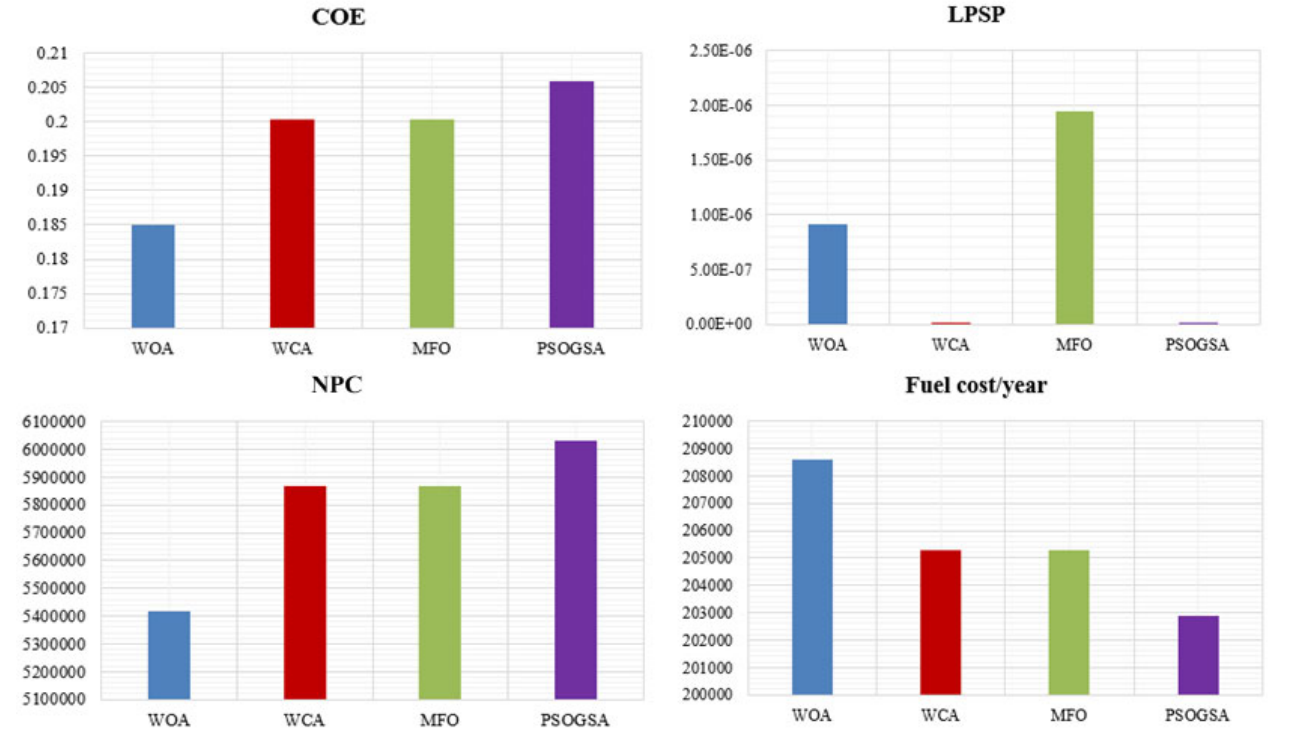

FIGURE 15. Comparison of the optimization parameters of the used optimization techniques.

The results show that the WOA optimization method can capable to reach the minimum best optimal value of the objective function. Base on the results, a note should be highlighted, the PSOGSA is faster than the other three algorithms according to the elapsed time (s) of the program operation for producing its optimal solution. However, this optimal solution is higher than that of the WOA. Therefore, the elapsed time and the attitude of objective functions of WOA and PSOGSA illustrate the superiority of WOA over PSOGSA to find the optimum minimum objective function in a small number of iterations as illustrated in Fig. 14 and Table 2. Moreover, in terms of acceptable

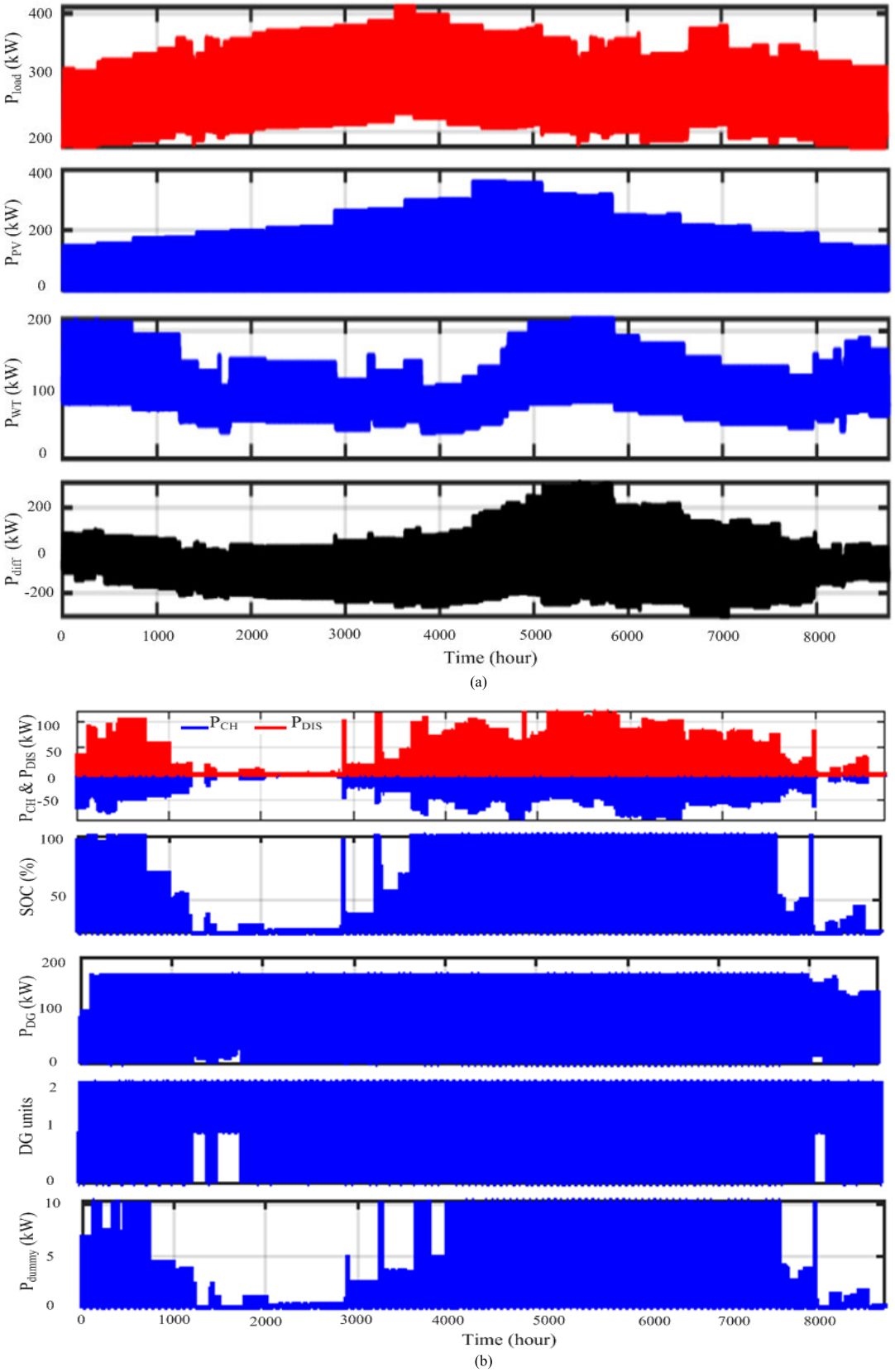

FIGURE 16. Simulation results of the optimal solution obtained from WOA for a one year of operation (i.e., 8760 hours).

solutions, the numerical results in tables and figures illustrate that the performance of WOA is faster and better compared to PSOGSA and other techniques.

Form the simulation results, it can be inferred that the WOA predicts the minimum COE of the system with the least NPC and LPSP within the predefined limits. Moreover, WOA predicts the best COE of 0.18500434 $/kWh, which results in a net present cost of 5418863.798$ and ensure the value of LPSP of 9.07269e-07, which agree with the predefined value ($<$0.04). The same results are obtained when the optimization algorithms are limited to 10 iterations, but unfortunately, all the proposed techniques did not reach the optimal final value for the cost function.

According to WOA algorithm, to ensure the minimum COE at the proposed location; 1400 PV modules, 15 wind turbines, (1.67941$\approx$ 2) DG units and 336 battery banks are estimated. Moreover, the COE obtained by WOA shows that the proposed hybrid microgrid system supply energy to the isolated village with an acceptable cost. The comparison is clearly presented in Fig. 15, in which the components of the objective function for each optimization method are presented.

Although WOA provides a minimal of COE, its fuel cost is the highest. The reason behind that can be clarified as that WOA gives the minimum value of battery storage units (i.e., 336 units), which forms a high cost of initialization and replacement. Accordingly, reducing the number of battery storage units leads to a reduction in COE. On the other side, decreasing the capacity of the storage system leads to a long operation of the diesel generator, which in turns consumes much fuel and raises the cost of fuel/year.

B. APPLICATION OF THE OPTIMAL CASE

Figure 16 shows the hourly variation of the generated power for the components of the proposed hybrid system at the optimum case of WOA. In this figure, the presented results are: the load demand (P_{load}), the total power generated from the renewable sources of energy (P_{PV}+P_{WT}), the generated power from the diesel units (P_{DG}), the number of diesel generator units in operation every hour (DG units), dummy load power (P_{dummy}), charge and discharge power of the storage battery system (P_{CH}&P_{DIS}), the state of charge of the battery bank system as percentage of the storage system capacity (SOC), and the fuel consumption of the diesel generator units. Due to the low wind speed in this area, the diesel generator units are daily operated with different degrees of generation to satisfy the demand for energy of the load during the hours of insufficient generation from the PV and wind turbine sources and low SOC for the battery system. While during the hours of high generation from the renewable sources the dummy load is operated to absorb the excess power over the demand of the load and the maximum limit of the storage system. For a better understanding of the energy management strategy behind the optimization algorithms, the daily simulation results of the hybrid system, taking into account the optimum operation conditions, are considered, as illustrated in Fig. 17.

Figure 17 shows the simulation results of WOA for a certain day (e.g., starting from time instant 3296 in Fig. 16) in summer. From Fig. 17(a), it is obvious that the daily load curve has two peaks, the first peak around 13:00 o'clock, where the temperature is very high and there is a need for reducing the air temperature using available air conditioners. The second peak is around 17:00 o'clock after the sunset, as all workers/farmers back home. During the night and early hours, the power generated from the renewable sources is minimum so that the diesel generator is working with high capacity (i.e. the two proposed DG units by WOA are working together). While after 06:00 o'clock, when the sun rises and the output power from PV and wind turbines increases, only one DG unit in conjunction with renewable sources are enough to satisfy the demand of energy. During daytime between 12:00 and 17:00 o'clock when the power generated from the nontraditional sources is greater than the load demand, the DG is switched off. Consequently, the excess power is used to charge the battery banks as shown in Fig. 17(b). The battery starts charging until reaching its maximum allowable limit. Moreover, when the battery is fully charged as given by the SOC of the battery when reaches 100%, the excess power is consumed in the dummy load, as given in Fig. 17(b). After sunset, the battery starts to discharge its energy until reaching the SOC_{min} and the DG starts to work again.

IX. STATISTICAL ANALYSIS

In this part, a detailed statistical analysis has been presented to provide a good explanation and assessment of the simulation results obtained by applying the proposed optimization techniques. Moreover, the performance stability of each proposed algorithm was tested in accordance with the application of sensitivity analysis. The present statistical study included, the maximum value of cost function, the minimum value, Mean value, Median, the Standard Deviation (SD), the Relative Error (RE), Root Mean Square Error (RMSE), Mean Absolute Error (MAE), and efficiency. These metrics have been evaluated as described in the following formulas:

$$SD = \sqrt{\frac{\sum_{i=1}^{n_R} \left(F_i - \bar{F}\right)}{n_R - 1}} \tag{62}$$

$$RE = \frac{\sum_{i=1}^{n_R} \left(F_i - F_{\min}\right)}{F_{\min}} \tag{63}$$

$$MAE = \frac{\sum_{i=1}^{n_R} \left(F_i - F_{\min}\right)}{n_R} \tag{64}$$

$$RMSE = \sqrt{\frac{\sum_{i=1}^{n_R} \left(F_i - F_{\min}\right)^2}{n_R}} \tag{65}$$

$$efficiency = \frac{F_{\min}}{F_i} \times 100\% \tag{66}$$

where F_i refers to the cost function for each of the proposed techniques at each run, F_{min} is the minimum recorded value of the objective function, and n_R refers to the number of runs of the MATLAB model. To achieve this study and evaluate

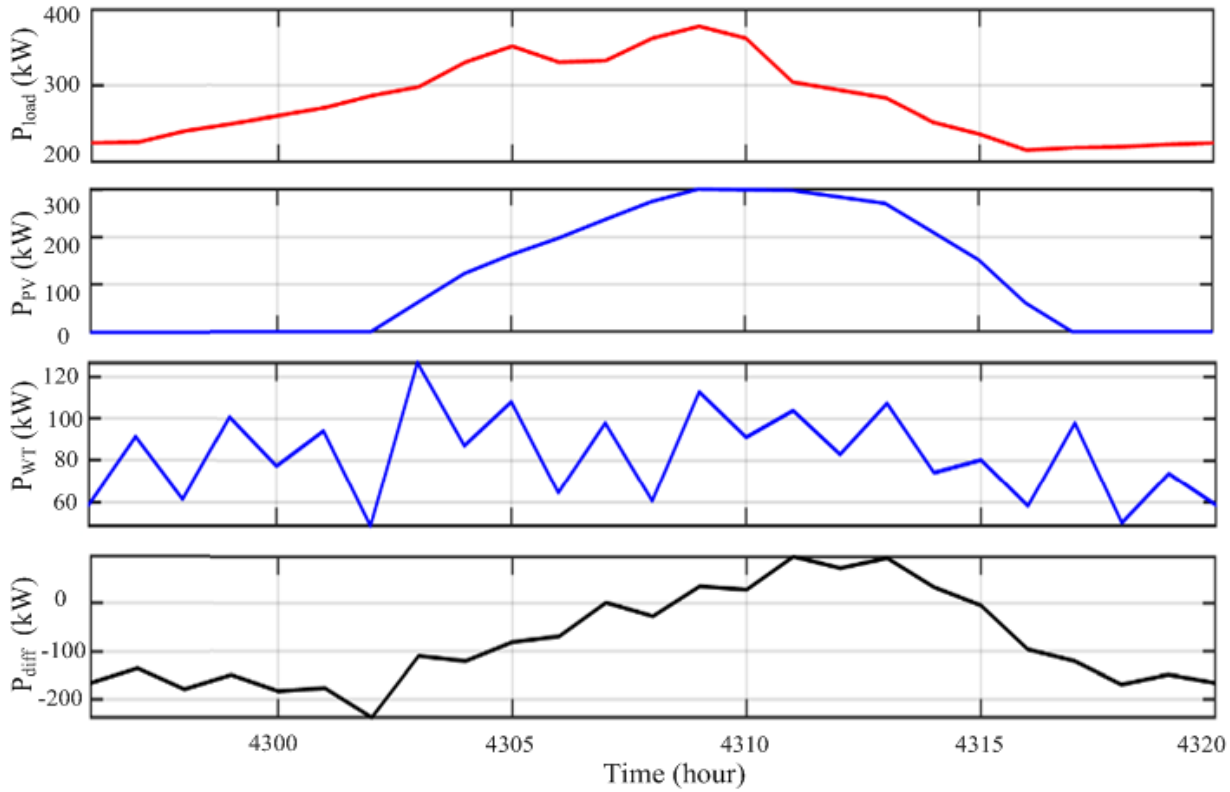

(a)

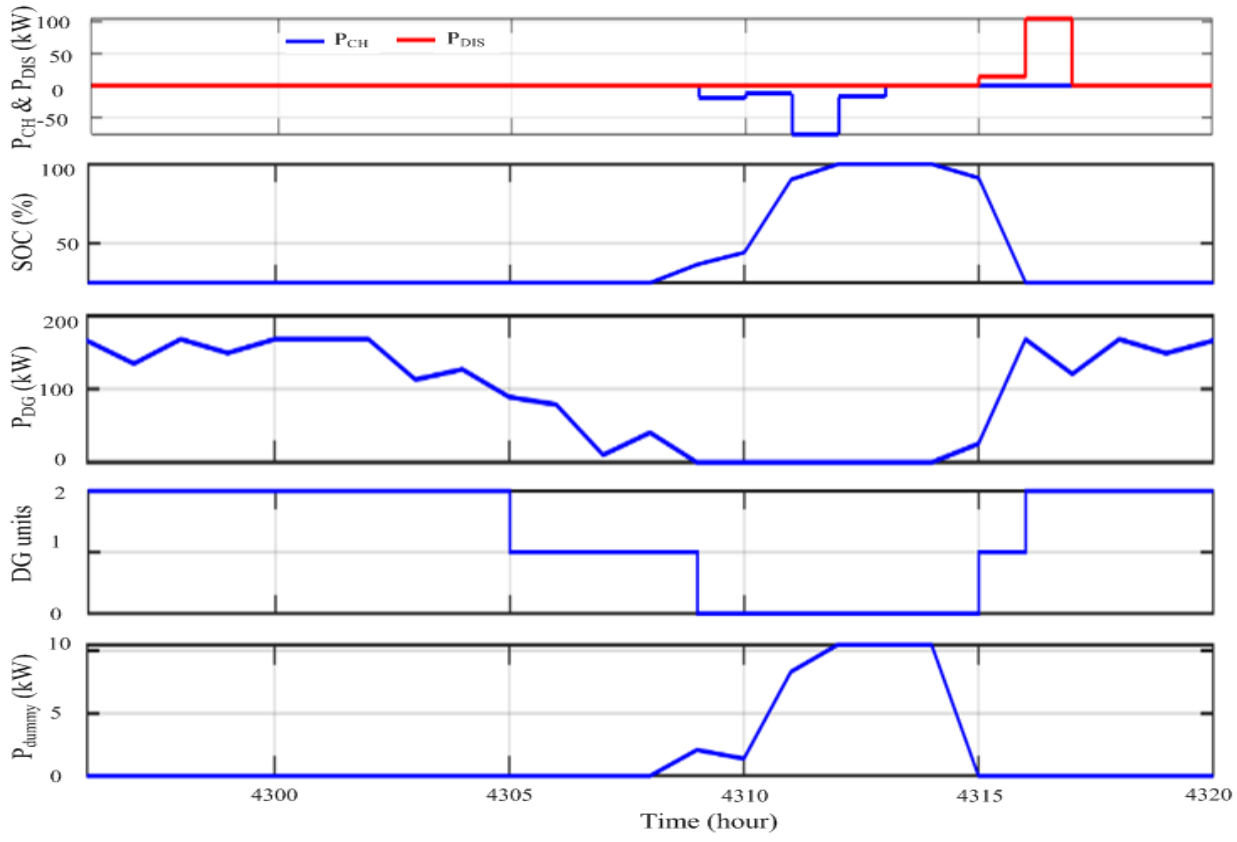

(b)

FIGURE 17. Simulation results with WOA of a certain day of operation in summer (i.e., 24 hours of operation between the instant of 4296 hour to 4320 hour).

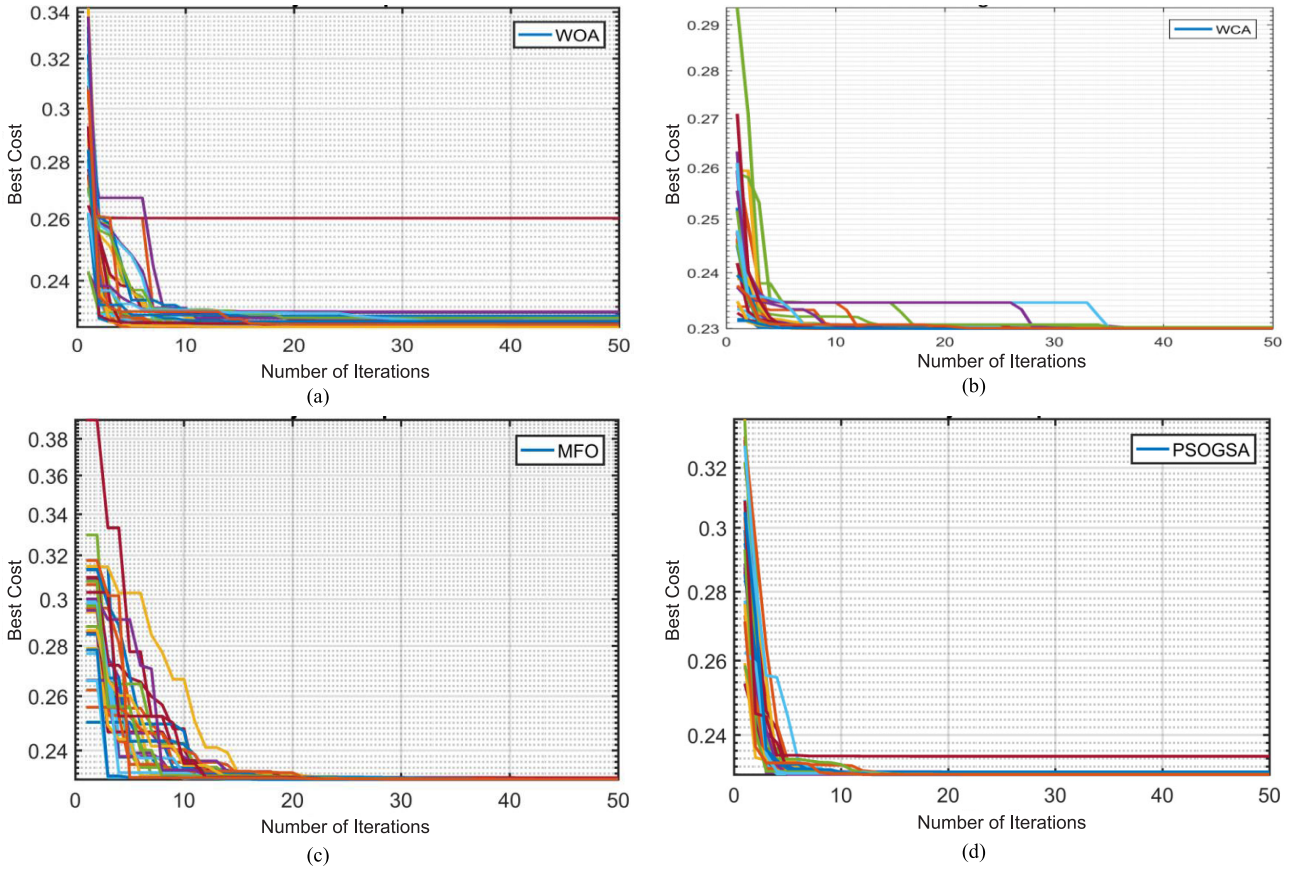

FIGURE 18. Convergence curves of the proposed optimization techniques considering 30 executions; (a) WOA, (b) WCA, (c) MFO, (d) PSOGSA.

TABLE 2. Optimization parameters of the proposed optimization techniques

		After 10 Iterations				Optimal Solution			
		WOA	WCA	MFO	PSOGSA	**WOA**	WCA	MFO	PSOGSA
Best objective function		0.226577	0.2301138	0.2337865	0.23010892	**0.2288333**	0.2299526	0.2299518	0.2300715
Best solution	PV	1400	1400.1460875	1400	1400	**1400**	1400	1400	1400
	Wind	15	15	15.0655	15	**15**	15	15	15
	DG	1.584727	1.59624	1.522534	1.59657	**1.679414**	1.629964	1.629922	1.598077
	Battery	589.4163	545.8431	572.8245	547.49001	**336.0255**	439.77882	439.8286	539.991
No. of iterations for optimal solution		---	---	---	---	**23**	16	41	14
COE ($/kWh)		0.198618	0.206216	0.2050342	0.2036462	**0.1850043**	0.2003754	0.2003736	0.205903
NPC ($)		5817622.382	6040150.480	6005547.529	5964894.825	**5418863.799**	5869088.725	5869036.077	6030997.822
LPSP		0.00009516	0.0000227	0.00587360	0.00545489	**$9.0726*10^{-7}$**	$8.482*10^{-13}$	$1.9451*10^{-6}$	$2.7977*10^{-10}$
Fuel cost		201779.714	202709.376	195983.612	197884.295	**208573.453**	205289.298	205286.098	202876.468
Dummy load (kWh)		14734.13601	15096.87249	15881.75126	15058.15653	**15483.097892**	14770.9425	14980.13723	14771.02531

TABLE 3. Evaluation of the statistical performance of the proposed optimization techniques

Technique	Max.	Min.	Average	Median	SD	Average RE	MAE	RMSE	Efficiency
WOA	0.2603056	0.2259942	0.2285081	0.22685783	0.61856738	0.33370396	0.002513839	0.00658076988	98.96218836
WCA	0.2306855	0.2299516	0.2300958	0.23002353	0.02187313	0.01880892	0.000144171	0.00025890931	99.93743000
MFO	0.2305667	0.2299516	0.2300366	0.22997916	0.01495997	0.01108690	0.000084981	0.00016987050	99.96309810
PSOGSA	0.2345954	0.2299516	0.2302699	0.23002350	0.08543884	0.04152667	0.000318304	0.00089831210	99.86307644

the performance of the proposed algorithm, the following parameters have been chosen as follows: search agents, number of iterations in each run and number of executions for the proposed algorithm are set to 10, 50, and 30, respectively. The convergence curves of proposed methods over the 30 executions are shown in Fig. 18. The statistical

performance for WOA, WCA, MFO, and PSOGSA is summarized in Table 3. As presented in Table 3, the WOA optimization algorithm has an acceptable RMSE. In addition, the value of SD proved that there is no change in the obtained results over the operation circle, which in turn manifests the stability of the proposed algorithm.

X. CONCLUSION

Implementation of a hybrid microgrid system can be considered as the optimum solution for electrification in rural and isolated regions. Considering the meteorological data of the site, a simulation model for describing the operation of a hybrid microgrid system, based on PV/wind/diesel and battery storage, has been investigated. In this study, four optimization techniques are proposed to obtain the optimum design of an isolated hybrid microgrid system. The goal of this work is to cover the load demand of the proposed location with the minimum cost of energy and high reliability of the power supply. A comprehensive comparison study between WOA, WCA, MFO, and PSOGSA is presented, while WOA presented high operation efficiency which appeared in the best COE and speed of convergence. Moreover, statistical and sensitivity analysis have been applied to evaluate the performance and test the stability of the proposed optimization techniques. Statistical results and simulation analysis concluded that WOA is the most promising among the proposed methods in solving the optimization problem. In fact, this study is useful for the decision-makers of New Valley, Egypt to think about the implementation of such hybrid systems as a convenient solution for electrification to reduce dependency on fossil fuels.

REFERENCES

[1] A. Evans, V. Strezov, and T. J. Evans, "Assessment of sustainability indicators for renewable energy technologies," *Renew. Sustain. Energy Rev.*, vol. 13, no. 5, pp. 1082–1088, 2009.

[2] P. Asmus, "Why microgrids are moving into the mainstream: Improving the efficiency of the larger power grid," *IEEE Electrific. Mag.*, vol. 2, no. 1, pp. 12–19, Mar. 2014. doi: 10.1109/MELE.2013.2297021.

[3] T. Ma, H. Yang, and L. Lu, "A feasibility study of a stand-alone hybrid solar–wind–battery system for a remote Island," *Appl. Energy*, vol. 121, pp. 149–158, May 2014.

[4] The Arab Republic of Egypt, Ministry of Electricity and Energy. *Egyptian Electricity Holding Company—Annual Report 2015-2016*. Accessed: Aug. 25, 2019. [Online]. Available: http://www.moee.gov.eg/english_new/report.aspx

[5] *The Official Website of the Ministry of Electricity and Energy*. Accessed: Sep. 21, 2018. [Online]. Available: http://www.moee.gov.eg

[6] H. M. Sultan, O. N. Kuznetsov, and A. A. Z. Diab, "Site Selection of large-scale grid-connected solar PV system in Egypt," in *Proc. EIConRus*, Moscow, Russia, Jan./Feb. 2018, pp. 813–818.

[7] E. R. Shouman, E. T. El Shenawy, and N. M. Khattab, "Market financial analysis and cost performance for photovoltaic technology through international and national perspective with case study for Egypt," *Renew. Sustain. Energy Rev.*, vol. 57, pp. 540–549, May 2016. doi: 10.1016/j.rser.2015.12.074.

[8] M. A. H. El-Sayed, "Substitution potential of wind energy in Egypt," *Energy Policy*, vol. 30, no. 2, pp. 681–687, Jun. 2002. doi: 10.1016/S0301-4215(02)00030-7.

[9] J. L. Bernal-Agustín, R. Dufo-López, and D. M. Rivas-Ascaso, "Design of isolated hybrid systems minimizing costs and pollutant emissions," *Renew. Energy*, vol. 31, no. 14, pp. 2227–2244, 2006.

[10] R. Dufo-López, J. L. Bernal-Agustín, J. M. Yusta-Loyo, J. A. Domínguez-Navarro, I. J. Ramírez-Rosado, J. Lujano, and I. Aso, "Multi-objective optimization minimizing cost and life cycle emissions of stand-alone PV–wind–diesel systems with batteries storage," *Appl. Energy*, vol. 88, no. 11, pp. 4033–4041, Nov. 2011.

[11] H. Yang, W. Zhou, L. Lu, and Z. Fang, "Optimal sizing method for stand-alone hybrid solar–wind system with LPSP technology by using genetic algorithm," *Solar Energy*, vol. 82, pp. 354–367, Apr. 2008. doi: 10.1016/j.solener.2007.08.005.

[12] B. O. Bilal, V. Sambou, P. A. Ndiaye, C. M. F. Kébé, and M. Ndongo, "Optimal design of a hybrid solar-wind-battery system using the minimization of the annualized cost system and the minimization of the loss of power supply probability (LPSP)," *Renew. Energy*, vol. 35, no. 10, pp. 2388–2390, 2010. doi: 10.1016/j.renene.2010.03.004.

[13] S. M. M. Tafreshi, H. A. Zamani, S. M. Ezzati, M. Baghdadi, and H. Vahedi, "Optimal unit sizing of distributed energy resources in microgrid using genetic algorithm," in *Proc. ICEE*, Isfahan, Iran, May 2010, pp. 836–841.

[14] M. Pirhaghshenasvali and B. Asaei, "Optimal modeling and sizing of a practical hybrid wind/PV/diesel generation system," in *Proc. 5th Power Electron., Drive Syst. Technol. Conf. (PEDSTC)*, Tehran, Iran, Feb. 2014, pp. 506–511.

[15] M. Bashir and J. Sadeh, "Optimal sizing of hybrid wind/photovoltaic/battery considering the uncertainty of wind and photovoltaic power using Monte Carlo," presented at the 11th Int. Conf. Environ. Elect. Eng. (EEEIC), Venice, Italy, May 2012.

[16] A. Navaeefard, S. M. M. Tafreshi, M. Barzegari, and A. J. Shahrood, "Optimal sizing of distributed energy resources in microgrid considering wind energy uncertainty with respect to reliability,"presented at the IEEE Int. Energy Conf. Exhib. (EnergyCon), Manama, Bahrain, Dec. 2010.

[17] O. Ekren and B. Y. Ekren, "Size optimization of a PV/wind hybrid energy conversion system with battery storage using simulated annealing," *Appl. Energy*, vol. 87, no. 2, pp. 592–598, 2010. doi: 10.1016/j.apenergy.2009.05.022.

[18] O. Ekren and B. Y. Ekren, "Size optimization of a PV/wind hybrid energy conversion system with battery storage using response surface methodology," *Appl. Energy*, vol. 85, no. 11, pp. 1086–1101, Nov. 2008.

[19] A. Crăciunescu, C. Popescu, M. Popescu, and L. M. Florea, "Stand-alone hybrid wind-photovoltaic power generation systems optimal sizing," presented at the 11th Int. Conf. Numer. Anal. Appl. Math. (ICNAAM), Rhodes, Greece, Sep. 2013.

[20] A. K. Kaviani, H. R. Baghaee, and G. H. Riahy, "Optimal sizing of a stand-alone wind/photovoltaic generation unit using particle swarm optimization," *Simulation*, vol. 85, no. 2, pp. 89–99, Feb. 2009. doi: 10.1177/0037549708101181.

[21] H. R. Baghaee, M. Mirsalim, G. B. Gharehpetian, and H. A. Talebi, "Reliability/cost-based multi-objective Pareto optimal design of stand-alone wind/PV/FC generation microgrid system," *Energy*, vol. 115, pp. 1022–1041, Nov. 2016. doi: 10.1016/j.energy.2016.09.007.

[22] H. R. Baghaee, M. Mirsalim, and G. B. Gharehpetian, "Multi-objective optimal power management and sizing of a reliable wind/PV microgrid with hydrogen energy storage using MOPSO," *J. Intell. Fuzzy Syst.*, vol. 32, no. 3, pp. 1753–1773, Jan. 2017. doi: 10.3233/JIFS-152372.

[23] A. Arabali, M. Ghofrani, M. Etezadi-Amoli, and M. S. Fadali, "Stochastic performance assessment and sizing for a hybrid power system of solar/wind/energy storage," *IEEE Trans. Sustain. Energy*, vol. 5, no. 2, pp. 363–371, Apr. 2014.

[24] M. A. Mohamed, A. M. Eltamaly, A. I. Alolah, and A. Y. Hatata, "A novel framework-based cuckoo search algorithm for sizing and optimization of grid-independent hybrid renewable energy systems," *Int. J. Green Energy*, vol. 16, no. 1, pp. 86–100, Oct. 2018. doi: 10.1080/15435075.2018.1533837.

[25] M. A. M. Ramli, H. R. E. H. Bouchekara, and A. S. Alghamdi, "Optimal sizing of PV/wind/diesel hybrid microgrid system using multi-objective self-adaptive differential evolution algorithm," *Renew. Energy*, vol. 121, pp. 400–411, Jan. 2018.

[26] V. Raviprabakaran and S. Ramachandradurai, "Optimal sitting of PV-wind-energy storage system integrated micro grid using artificial bee colony optimization technique," *Int. J. Innov. Res. Comput. Commun. Eng.*, vol. 5, no. 5, pp. 9640–9652, 2017.

[27] M. S. Ngan and C. W. Tan, "Assessment of economic viability for PV/wind/diesel hybrid energy system in Southern Peninsular Malaysia," *Renew. Sustain. Energy Rev.*, vol. 16, no. 1, pp. 634–647, Jan. 2012.

[28] A. M. A. Haidar, P. N. John, and M. Shawal, "Optimal configuration assessment of renewable energy in Malaysia," *Renew. Energy*, vol. 36, no. 2, pp. 881–888, Feb. 2011.
[29] *Wind Turbines—Part 3: Design Requirements for Offshore Wind Turbines*, 1st ed., Standard IEC 61400-3:2009, Geneva, Switzerland, 2009.
[30] M. S. Ismail, M. Moghavvemi, and T. M. I. Mahlia, "Techno-economic analysis of an optimized photovoltaic and diesel generator hybrid power system for remote houses in a tropical climate," *Energy Convers. Manage.*, vol. 69, pp. 163–173, May 2013.
[31] R. Dufo-López, J. L. Bernal-Agustín, J. M. Yusta-Loyo, J. A. Domínguez-Navarro, I. J. Ramírez-Rosado, J. Lujano, and I. Aso, "Multi-objective optimization minimizing cost and life cycle emissions of stand-alone PV–wind–diesel systems with batteries storage," *Appl. Energy*, vol. 88, no. 11, pp. 4033–4041, Nov. 2011.
[32] A. Kaabeche, M. Belhamel, and R. Ibtiouen, "Optimal sizing method for stand-alone hybrid PV/wind power generation system," in *Proc. Revue Energies Renouvelables (SMEE)*, Bou Ismaïl, Tipaza, 2010, pp. 205–213.
[33] S. Mirjalili and A. Lewis, "The whale optimization algorithm," *Adv. Eng. Softw.*, vol. 95, pp. 51–67, May 2016. doi: 10.1016/j.advengsoft.2016.01.008.
[34] R. Masadeh, A. Alzaqebah, and A. Sharieh, "Whale optimization algorithm for solving the maximum flow problem," *J. Theor. Appl. Inf. Technol.*, vol. 96, no. 8, pp. 2208–2220, Apr. 2018.
[35] H. Eskandar, A. Sadollah, A. Bahreininejad, and M. Hamdi, "Water cycle algorithm—A novel metaheuristic optimization method for solving constrained engineering optimization problems," *Comput. Struct.*, vols. 110–111, pp. 151–166, Nov. 2012.
[36] A. Sadollah, H. Eskandar, A. Bahreininejad, and J. H. Kim, "Water cycle algorithm for solving multi-objective optimization problems," *Soft Comput.*, vol. 19, no. 9, pp. 2587–2603, Sep. 2015.
[37] S. Mirjalili and S. Z. M. Hashim, "A new hybrid PSOGSA algorithm for function optimization," in *Proc. ICCIA*, Tianjin, China, Dec. 2010, pp. 374–377.
[38] R. Eberhart and J. Kennedy, "A new optimizer using particle swarm theory," in *Proc. 6th Int. Symp. Micro Mach. Hum. Sci.*, Nagoya, Japan, Oct. 1995, pp. 39–43. doi: 10.1109/MHS.1995.494215.
[39] J. Kennedy and R. C. Eberhart, "Particle swarm optimization," in *Proc. 4th IEEE Int. Conf. Neural Netw.*, Piscataway, NJ, USA, Nov. 1995, pp. 1942–1948.
[40] E. Rashedi, H. Nezamabadi-Pour, and S. Saryazdi, "GSA: A gravitational search algorithm," *J. Inf. Sci.*, vol. 179, no. 13, pp. 2232–2248, 2009.
[41] S. Mirjalili, "Moth-flame optimization algorithm," *Knowl.-Based Syst*, vol. 89, pp. 228–249, Nov. 2015.
[42] M. A. Tolba, H. Rezk, V. Tulsky, A. A. Z. Diab, A. Y. Abdelaziz, and A. Vanin, "Impact of optimum allocation of renewable distributed generations on distribution networks based on different optimization algorithms," *Energies*, vol. 11, no. 1, p. 245, Jan. 2018.
[43] M. H. Sulaiman, Z. Mustaffa, M. I. M. Rashid, and H. Daniyal, "Economic dispatch solution using moth-flame optimization algorithm," in *Proc. MATEC Web Conf.*, Hongliang Yuan, China, vol. 214, 2018, p. 03007. doi: 10.1051/matecconf/201821403007.

AHMED A. ZAKI DIAB received the B.Sc. and M.Sc. degrees in electrical engineering from Minia University, Egypt, in 2006 and 2009, respectively, and the Ph.D. degree from the Electric Drives and Industry Automation Department, Faculty of Mechatronics and Automation, Novosibirsk State Technical University, Novosibirsk, Russia, in 2015. He received the Postdoctoral Fellowship from the Moscow Power Engineering Institute (MPEI), National Research University, Moscow, Russia, from 2017 to 2018. Since 2001, he has been with the Department of Electrical Engineering, Faculty of Engineering, Minia University, Egypt, as a Teaching Assistant, a Lecturer Assistant, and since 2015, as an Assistant Professor. He is currently a Visiting Researcher with Kyushu University, Japan, (received the MIF Postdoctoral Fellowship, in 2019). His present research interests include ac drives, renewable energy, smart-grids and optimization, and artificial intelligence.

HAMDY M. SULTAN received the B.Sc. degree in electrical power engineering and the M.Sc. degree in electrical engineering from Minia University, Minia, Egypt, in 2014. He is currently pursuing the Ph.D. degree with the Moscow Power Engineering Institute, National Research University, Moscow, Russia. The key research areas include power system plan and operation, power system transient stability, and renewable energy.

IHAB S. MOHAMED received the B.S. degree from the Institute of Aviation Engineering and Technology (IAET), Egypt, in 2009, and the M.S. degree in electrical engineering from Cairo University, Egypt, in 2014. From 2015 to 2017, he was an M.Sc. student of European Master in Advanced Robotics (EMARO+). He attended the first year of EMARO+ at the Warsaw University of Technology (WUT), Poland, while the second year, he was at the University of Genoa (GU), Italy. He is currently pursuing the Ph.D. degree in robotics engineering at INRIA Sophia Antipolis - Méditerranée, Université Côte d'Azur, France, under the supervision of Prof. P. Martinet, G. Allibert, and P. Salaris.

From 2009 to 2015, he was a Teaching Assistant with the Electronics and Communications Department, IAET. His research interests include predictive control (MPC), power electronics, robotics, computer vision, and machine learning.

KUZNETSOV OLEG N. received the B.Sc. and Ph.D. degrees in electrical power engineering from the Moscow Power Engineering Institute, National Research University, Moscow, Russia, in 1999 and 2003, respectively. He is currently with the Moscow Power Engineering Institute. He is a Co-chairman of the Scientific and Methodological Council in the direction of power and electrical engineering (electrical power module). His main research interests include power system planning, power system stability, distributed generation, and energy management of smart grids.

TON DUC DO (S'12–M'14) received the B.S. and M.S. degrees in electrical engineering from the Hanoi University of Science and Technology, Hanoi, Vietnam, in 2007 and 2009, respectively, and the Ph.D. degree in electrical engineering from Dongguk University, Seoul, South Korea, in 2014.

From 2008 to 2009, he was with the Division of Electrical Engineering, Thuy Loi University, Vietnam, as a Lecturer. He was with the Division of Electronics and Electrical Engineering, Dongguk University, as a Postdoctoral Researcher, in 2014. He was also a Senior Researcher with the Pioneer Research Center for Controlling Dementia by Converging Technology, Gyeongsang National University, South Korea, from 2014 to 2015. Since 2015, he has been an Assistant Professor with the Department of Robotics and Mechatronics, Nazarbayev University, Kazakhstan. His research interests include advanced control system theories, electric machine drives, renewable energy conversion systems, uninterruptible power supplies, electromagnetic actuator systems, targeted drug delivery systems, and nanorobots.

Dr. Do received the Best Research Award from Dongguk University, in 2014. He was the Lead Guest Editor of the special issue of *Mathematical Problems in Engineering* on Advanced Control Methods for Systems with Fast-Varying Disturbances and Applications. He is currently an Associate Editor of IEEE Access.